

**INVESTIGATION OF EFFECT OF NANOCRYSTALLIZATION
ON MECHANICAL AND SHAPE MEMORY EFFECT OF CuZnAl
BASED SHAPE MEMORY ALLOY, SYNTHESIZED BY HIGH
ENERGY BALL MILLING (HEBM)**

A DISSERTATION

*Submitted in partial fulfillment of the
requirements for the award of the degree*

of

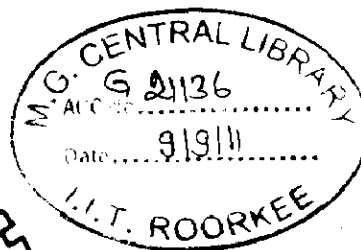
MASTER OF TECHNOLOGY

in

NANOTECHNOLOGY

By

SUJIT KUMAR VERMA



**CENTRE OF NANOTECHNOLOGY
INDIAN INSTITUTE OF TECHNOLOGY ROORKEE
ROORKEE - 247 667 (INDIA)**

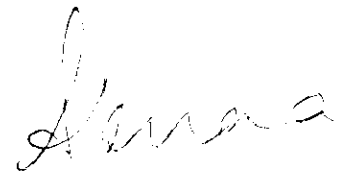
JUNE, 2011

DECLARATION OF THE CANDIDATE

I hereby declare that the work being presented here entitled “Investigation of the effect of nanocrystallization on mechanical and Shape Memory Effect of shape memory alloy synthesized by High Energy Ball Milling (HEBM).” Is an authentic record of my own work under the guidance of Dr B.S.S.Daniel, Associate Professor, Department of Metallurgical and Materials Engineering, IIT Roorkee. The matter presented in this report to the best of my knowledge has been never presented for the award of any other degree elsewhere.

June 30, 2011

Place: I I T Roorkee



Sujit Kumar Verma

ACKNOWLEDGEMENT

I wish to express my deep sense of gratitude and sincere thanks to my guide **Dr. B.S.S. Daniel, IIT Roorkee**. For being a great source of inspiration. His keen interest, active. Enthusiastic support, analytical suggestions has been a great driving force behind all my efforts. I wish to extend my sincere thanks for his excellent guidance and suggestions for successful completion of my dissertation work.

My heartily thanks to **Prof. (Mrs.) Vijaya Agarwala** for readily permitting me to use (HEBM) facility of her lab and also for her suggestions for precautionary measures.

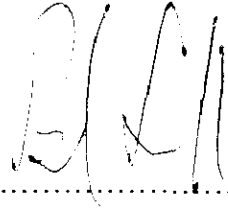
I also thank to head IIC Roorkee and technical staff. For cooperation and support in using characterization facilities, Xrd, SEM, FE-SEM and DTA/TGA.

My thanks to technical staff of MMED labs, Nanotech labs for their cooperation and support

At last my thanks to all my friends who helped me, throughout the work by their valuable suggestions.

CERTIFICATE

This is to certify that report submitted by Mr. Sujit Kumar Verma on “Investigation of effect of Nanocrystallization on mechanical and shape memory effect of shape memory alloy Cu₇₄ Zn₂₂Al₄(wt%) synthesized by High Energy Ball Milling (HEBM) for partial fulfillment of the award of degree of M.Tech, is an authentic record of his dissertation work, which he satisfactorily completed under my supervision.



Dr. B.S.S. Daniel

Associate Professor

I.I.T Roorkee

Abstract

Present work is based on synthesis of shape memory nano-alloy by mechanical alloying using high energy ball mill. Shape memory alloys are very useful in various applications, especially in actuators, smart systems, and medical applications. These materials recognize their shape due to the pseudo-elastic property they exhibit. Pseudo-elastic transformation itself is not a naturally occurring phenomenon. Instead, it can be achieved by thermo mechanical training. Shape memory effect shown by alloys depends upon its constitution, method of preparation and thermo mechanical training. Method of preparation has been the most important aspect for shape memory alloys for achieving desired SME (shape memory effect). Earlier works done by most of the authors on shape memory effect were based on conventional method of synthesis i.e. casting and powder metallurgy routes. These methods do not emphasize on effect of nanocrystalline phase on shape memory effect and fatigue strength of devices based manufactured from shape memory effect. In the present work we have focused on synthesis of shape memory alloy by mechanical alloying using high energy ball mill. Several process parameters such as, ball to powder ratio, milling medium, and speed of ball mill are important factors which influence effectiveness of the milling process. By selecting proper ball to powder ratio, rotational speed and medium of milling, one can optimize the milling and alloying process. In our work we have chosen powder Cu, Zn and Al of known proportion of size 325 mesh and purity greater than 99.7%, ball to powder ratio of 3:1 and the planetary ball mill was maintained at 300 rpm. In first case we milled the powder up to 24 hours dry milling and taken out samples for XRD (X-Ray Diffraction), SEM (Scanning Electron Microscopy), DSC (Differential Scanning Calorimetry) analysis in order to know about physical and morphological changes occurring with milling time and phase transformation changes can be analyzed by XRD and DTA/TGA (Differential Temperature Analysis/Temperature Gravimetric Analysis) test.

We have found that when liquid nitrogen used at 24 hour milled state there has been drastic decrease of particle size, earlier up to 24 hour milling decrease in particle size has small and gradual. From 24 to 28 hour milling with liquid nitrogen, reduction in particle size was max, no further reduction of particle size was observed, in fact there has been increase of grain size observed due to agglomeration and grain growth due to evolved heat. In second set of sample we added liquid nitrogen at 16 hour stage and milled up to 20 hour and found that reduction of particle size was same as it was in earlier sample. FE-SEM (Field Emission-Scanning Electron Microscopy) .AND DSC analysis also conforms the results. Particle size reduction up to 7 nanometers was observed in optimize state. Micro hardness test shows increase of hardness and yield strength with decrease of particle size up to 15 nanometers and then reverse effect observed. Adequate yield strength and fatigue strength are most important properties of shape memory alloys in order to perform its role efficiently. To achieve desired property particle size control is most important aspect. Mechanical alloying by HEBM is the most competitive technique because we have complete control over morphological changes by controlling over milling parameters.

Contents

Title	Page No
Chapter 1: Introduction	1
1.2 SMAs	3
1.3 SME Types	5
1.4 Characterization Techniques	10
1.5 Fabrication Techniques	11
1.6 Formation of Nanostructures by HEBM	12
1.7 Applications of SMAs & Smart materials	15
Chapter 2: Literature Review	18
Chapter 3: Experimental Methods	23
3.1 X-Ray Diffraction	23
3.2 SEM (Scanning Electron Microscopy)	25
3.3 FE-SEM and EDAX	27
3.4 Optical Metallography	33
3.9 DTA/DTG Analysis	35
Chapter 4: Results and Discussion	37
4.1 X-Ray Diffraction Analysis	38
4.4 SEM& FE-SEM	42-45
4.6 EDAX	46
4.7 FE-SEM and EDAX sintered pellets	53
4.11 Optical Metallography	61
4.11a DTA/DTG Analysis	63
Chapter 5: Conclusion and further work	76
Chapter 6: References	77

INDEX: FIGURES AND TABLES

Title	Page No
Fig: 1.2 A phenomenological description with two martensite	7
1.3 One way shape memory	8
1.6 Stress strain curve	11
1.7 Schematic Sketch of mechanical attrition	13
1.8 Mechanism of energy and power generation	17
3.1 View of Bruker D-8 X-RD Machine at IIC	23
3.2 SEM System at IIC	25
3.3 Schematic diagram- main component of SEM	26
3.4 FE-SEM & EDAX System at IIC	27
3.5 FE-SEM Schematic working principle	28
3.6 Hydraulic press at Nanotech lab IITR	30
3.7 Green Pellets	30
3.8 Sintered Pellets	31
3.9 Microhardness Schematic Diagram	31
3.10 Hot Rolling Machine	32
3.11 Mounted Sample	34
3.12 Optical Microscope	34
3.13 Thermal Analyzer	35
4.1 Cu Powder XRD	36
4.2 Zn Powder XRD	37
4.3 Al Powder XRD	37
Table: 4.2 Variation of lattice parameter	37
4.4 XRD patterns of group samples	38
4.4(a, b, e, f, g, h) SEM pictures	42
4.5 FE-SEM pictures	45

4.6 (a) EDAX 2 hr milled sample	46
4.6(b) EDAX selected area	47
4.6(c) EDAX 16 hr	48
4.6(d) EDAX Pattern 34 hr milled selected area	49
4.6(e) EDAX 28 hr selected area	50
4.6(f) EDAX 40 hr selected area	51
4.7 (a) FE-SEN of sintered pellets	53
4.7(b) EDAX selected area as mixed powder	54
4.7(c) EDAX 2 hr milled	55
4.7(d) EDAX of 20 hr milled	56
4.7(e) EDAX of 48 hr milled	57
4.8 Density/milling time graph	58
4.9 Microhardness v/s milling hrs graph	59
4.11(a, b, c, d) Optical Micrograph	61-62
4.11(a, b) DTA/DTG graph	63
Table: Transition Temperature for DTG curves	66
4.11© DTG-Time analysis	67
4.11(a) Phase transformation states	68
Table: 4.1 Phase Transformations Temp.	68
Table: 4.2 Temperature Difference Table	69
4.11(e) DTA-multiple plot	70
4.11(f, g) DTA multiple heating plot	72
4.11(g) DTG Temp multiple heating plot	73
4.11(i) Phase Transition states	74
Table: Phase Transformation Temperature	74
Table: 4.1(j) Phase Temperature Difference Table	75

Chapter: 1 Introduction

1.1 In recent years, Cu based shape memory alloys have emerged as a replacement of widely used Ni-Ti alloys, due to their comparable recovery force, lower material cost, and relative ease of processing. The potential application area of Cu based shape memory alloys has been identified in various electrical equipment, green houses windows as actuators and sensors. Among Cu based shape memory alloys, Cu Zn Al alloy have been found to be promising candidate. At an international scale the shape memory alloys (SMA) used mainly for commercial purposes belong to the Ni-Ti or copper based (Cu-Zn-Al) and (Cu-Al-Ni) systems. The Cu-Zn-Al alloys stay on the second place due to the higher characteristics of Ti based alloys in different applications. Yet taking into account the very high price (about 1\$/g) of Ni-Ti alloys, the Cu based alloys remain a good economic alternative, due to their price 100 times lower [1,2] in addition to above economic advantages, Cu-Zn-Al alloys exhibits, about 6% shape memory effect or 2% two way shape memory effect (TWSME) [3,4]. A 1 j/g mechanical work developed by heating, as well as pseudo elastic change. However, Cu-Zn-Al alloys produced by conventional casting route are quite brittle, which limits its applicability. It has been pointed out that high brittleness of Cu-Zn-Al alloys is primarily related to the large elastic anisotropy and large grain size, which enhance the susceptibility of alloys to intergranular fracture [5, 6]. In pursuit of improving mechanical properties, several attempts have been made to refine grain size of Cu-Zn-Al alloys by adding various alloying elements, such as Ti, Zr, V and boron [7, 8]

Grain size refinement exhibited significant improvement in the mechanical properties as compared to coarse-grained alloys. However, the problem of composition control during casting, which is crucial for controlling the transformation temperature and desired level of grain refinement, has hindered its further development. It is well established that the grain size and composition can be controlled in materials produced by powder metallurgy route in

better way. In particular mechanical alloying has emerged as a promising method to produce a variety of nanocrystalline and ultra fine grained powders. Alloy powders produced by mechanical alloying have shown to possess better control over composition and chemical homogeneity as compared to their conventionally produced counterparts.

In recent years few attempts have been made to develop Cu-Zn-Al alloys by a powder metallurgy route involving mechanical alloying followed by consolidation of milled powder via hot extrusion or isostatic pressing at elevated temperature [9, 10]. Since micro structural evolution in consolidated material is derived from the mechanically alloyed powders, it is extremely important to acquire an in-depth understanding of the structural evolution in the Cu-Zn-Al powder during mechanical alloying. However very little attention has been focused to this aspect in the literature.

The present work describes the experimental results related to micro structural evolutions, such as particle size, and phase evolution during different stages of mechanical alloying of $\text{Cu}_{74}\text{Zn}_{22}\text{Al}_4$ (Wt %) powder mixture. A detailed analysis of the milled nano-crystalline powder was carried out by TEM for observing the nano-scale features present inside the mechanically alloyed powder particles.

The mechanism related to shape memory effect (SME) are essentially governed by the occurrence of preferred microstructure constitution of martensite and parent phase involved in the reversible transformations cycles [11, 12].

It has been established that Cu-based shape memory alloys(SMAs) conform to many of the commercial and technological necessities like affordable cost, favorable deformation behavior and better electrical and thermal conductivities[13].

However repetitive transformation cycles in such alloys results into accumulated chemical and topological changes resembling the attributes of isothermal ageing process [14, 15].

Moreover formation of the precipitate phases during the ageing treatment significantly contributes to the profile of the hysteresis loop [16] as well as appearance of two-way shape memory effect [17].

Moreover, the accumulated interface migration during the reversible transformation cycling in SMAs, particularly in the presence of precipitate phase, may significantly influence the value of the percent recoverable strain yielded by the subsequent transformation cycle [13,14].

This may reasonably be attributed to the pinning of the migration interphase boundaries by precipitate phases [15, 16].

1.2 Shape Memory Alloys

Shape memory alloys and smart materials are relatively new class of materials with the unique property of SME (shape memory effect). These materials are becoming popular because of their **shape memory characteristics**, by which an article deformed at low temperature will revert to its original shape when heated to a higher temperature.

Smart materials are those materials which possesses sensing and actuation properties such as piezoelectric response to dynamic strain that causes electrons to move. Smart structures are smart materials for sensing and actuation in analogue or digital closed-loop feedback systems.

Some alloy systems exhibiting the shape memory effect are Ni-Ti, Cu-Zn-Al, Au-Cd [18, 19] and Ni-Al. Other interesting properties Ni-Ti based SMA are superelasticity and biocompatibility, which are useful in medical applications. **The unique ability of SMAs to remember and recover their original shape, combined with their energetic recovery power and precise shape-temp.-stress-magnetic response**, has stirred so much interest in these materials potential for defense and industrial applications. The Most currently used SMAs, including NiTi, Cu-Zn-Al, and Cu-Ni-Al have a phase transformation temp. below 100 deg. cel. This unfortunately hinders the application of the SMAs in high-temp environments, which are precisely where their application will be most useful. Many defense and industrial fields that employs shape controlling and vibration depression in high-temp. Environment would greatly benefit by using high-temp. SMAs.

Recently scientists have made inroads into research on newer, higher temperature SMAs that have a phase transformation temp. Much greater than that of the typically employed SMAs

Most of the research has focused on the (Ni_{50-x} X_x) Ti (x=Pd, Pt, Au) and Ni-Mn-Ti alloys systems because it is believed that to have the best potential.

Smart structures can also be passive such as wing designed with bend- twisting coupling to protect against flutter, or semi active, such as a magnetorheologic damper that uses a feedback to control voltage field and viscosity of a fluid

Although we are at early stage of research, nanoscale intelligent materials including carbon nanotube, inorganic nanotubes, compound nanotubes, nanobelts, and other nanoscale materials have produced great interest in the research field. This happens due to their remarkable and varied electrical and mechanical properties i.e. electrical conductance, high mechanical stiffness, light weight, electron spin resistance, electro-chemical actuation, piezoelectricity, piezoresistance, contact resistance, coulomb drag power generation, thermal conductivity, luminescence, and the possibilities for functionalizing these materials to change their intrinsic properties. These attractive properties also have potential to allow development of self-contained nanoscale intelligent materials based on analog or digital control of the material using built-in nanoscale electronics.

Emphasis is on nano-tube based materials that have novel strain sensing and force actuation properties and the associated material processing steps needed to build nanoscale materials from nanoscale components, including digital control of the material behavior. nanoscale smart materials are important **because they often possess improved or different properties from macroscale materials due to their near-perfect construction, large surface to volume ratio and quantum effect [18-19]** while nanoscale material, and in particular carbon nanotubes (CNTs), have extraordinary properties, utilizing these properties at the nanoscale and at the macroscale is presenting major challenges for scientist and engineers.

Nanoscale smart and intelligent materials are based on carbon nanotubes-(SWCNT) is a superelastic crystalline molecule that can have a length-to-diameter ratio of 1000 or more, and enormous interfacial area of $500\text{m}^2/\text{gm}$ or more. multifunctional materials are being designed by mixing nanotubes with bulk carrier materials is now producing a range of new properties such as:

- 1: piezoresistivity**
- 2: toughness**
- 3: electrochemical transduction**
- 4: thermal and electrical conduction**
- 5: enhanced modulus, hardness**

Controlling and using above mentioned properties for smart material is depends on understanding the composition, topography, and processing relationship that define nanomaterial behavior.

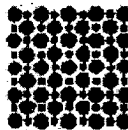
In the broadest sense, the goal of nanoscale materials research is to develop multifunctional smart materials. these material will possess high-strain- to-failure value and high stiffness, lightweight and possess high bandwidth for actuation or sensing.

These materials are being used as strong structural materials that simultaneously perform sensing, actuation, and other functional activities. Till now no other smart functional material available that is structural also therefore nanotube hybrid actuator and sensor materials could become an enabling technology for the improvement of all kinds of **dynamic systems including helicopters, reconfigurable aerodynamic surfaces, launch vehicles, ultra-high energy density wireless motors, and biomedical implants.** Nanotechnology is attractive and exciting because it may produce the most efficient smart materials ever made.

Large advances in nanoscale materials development have occurred. Recent trends are towards increasing percentage of CNT are being incorporated into polymers, carbon fibers, and metals for reinforcement, and these hybrid materials have shown significant improvement in elastic modulus or toughness, as compared to host polymer material

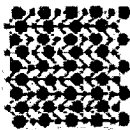
Austenite

- High temperature phase
- Cubic Crystal Structure



Martensite

- Low temperature phase
- Monoclinic Crystal Structure



Twinned Martensite



Detwinned Martensite

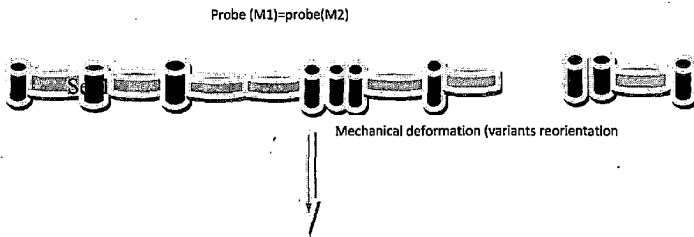
1.3 SHAPE MEMORY EFFECT (SME): TYPES

Smart materials exhibit shape memory effect. Most of the available SMAs show one way SME strongly, however some alloys also exhibit two way shape memory effect.

ONE WAY SHAPE MEMORY EFFECT: - “one way shape memory effect” happens when the material, previously deformed in martensite, recovers its original shape while heating up to austenite. Fig 1 illustrates an example of the SME. The graph on left side represents the stability zone for two phases on stress/temperature curves, the oblique lines denote the Clausius-Clapeyron relationship, indicating the boundary between phases and transition period. Consider a strip having flat shape as parent shape (i.e., “the memorized shape”) if stress is higher than a critical stress (σ_c) is applied, the strip can be deformed in a

plastic-like way (step 1). That means that the deformation applied on the material is stable in martensite. Upon heating (step-2) up to a critical temperature the material transforms to austenite and recovers its original shape, the parent shape. On cooling down (step-3), no more shape change is observed. Once again, a previous deformation in martensite is required to observe a macroscopic shape change. This is a reason why the term “one-way” is used to qualify the effect. Considering the macroscopic shape of the material, this effect is not recoverable, upon cooling. The material keeps its austenite shape.

The reason behind one way SME is that non oriented martensite is created upon cooling, and therefore martensite and austenite crystal structures are associated with same with the same specific macroscopic shape. A previous deformation in martensite is required to create a shape change while heating up to the austenite this phenomenon can be explained statistically, upon cooling martensite is randomly distributed, thus the resulting macroscopic deformation with respect to austenite shape is zero. The effect of deforming the material in martensite is to modify the variants distribution. fig 2 descriptions in on dimensions shows a simplified phenomenological description in one dimension with two martensitic variants symbolically represented by vertical and horizontal rectangle (M1, M2).



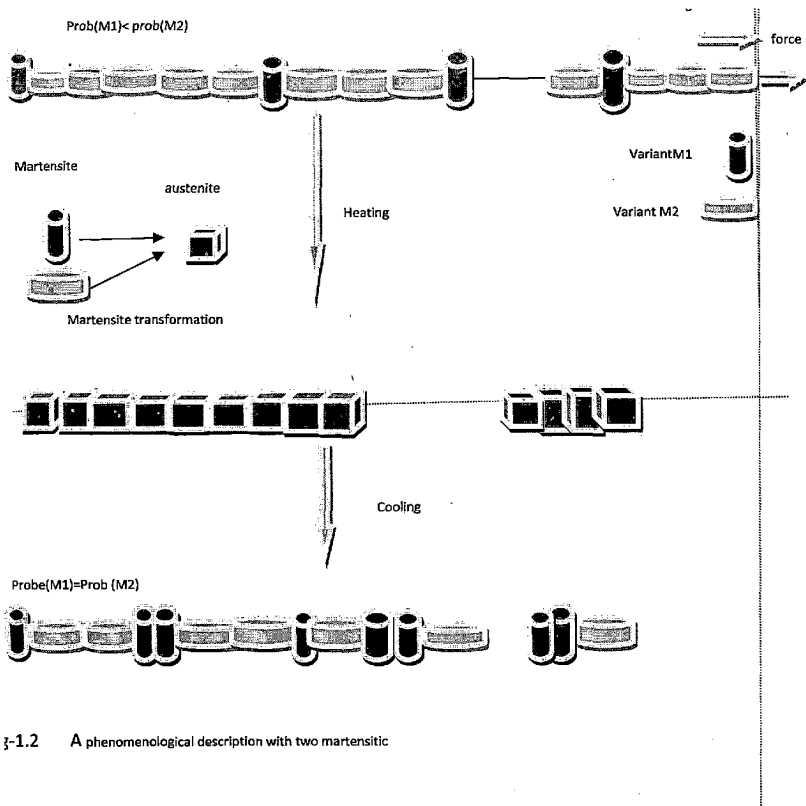


Fig-1.2 A phenomenological description with two martensitic

In this model, the material is, supposed to be free of any internal stress. With no stress applied on the model (set1), the martensite variants are randomly distributed: each variant has the same probability. When applying a force (set 2), the variants are reoriented in order to minimize the stress within the structure. The distribution between two variants is therefore modified. Upon heating, as the austenite –symbolically represented by a square – has a higher symmetry than martensite, the two martensitic variants are transformed into the same “crystallographic” structure. It does not matter in which configuration the material is in martensite (set1 or set2 for instance), the parents shape will be the same. Upon cooling (set4) , if no stress is applied , the two martensitic variants have the same probability, and therefore, the macroscopic shape will remain the same as the austenite shape.

TWO WAY SHAPE MEMORY EFFEC: two way shape memory alloys- (TWSMAs) can memorize two configurations, as opposed to one. The two ways memory effect became known in the mid -1970, a complete know-how of the mechanism of the phenomenon has yet not been completely explained even today. TWSMAs have shown immense potential for use in defense purposes and other industries due to their specific features. Typical potential applications include connectors for missile guidance systems, jet fighter hydraulic couplings, tank actuators, satellite components, as well as medical and robotics usage.

Recent literature reports that a few of current low-temperature SMAs, such as Ni-Ti, Cu-Al-Ni, and Cu-Zn-Al, can demonstrate two memory effects after proper Thermomechanical training. It is also reported .it is also reported that the two- way memory effect of these alloys strongly depends on the training procedures. However, there is little similar work that has been done on either one-way or two way memory effects of high temperature shape memory alloys (HTSMAs).

(a)HOW IT WORKS: phenomenon of SME is related to martensitic transformation, [1, 2, 7] the same transformation that may be used to harden the surface of steel.

In both steel and SMA, martensite forms on cooling of the alloy. Upon heating, martensite tempers in steel, changing its crystal structure, whereas in SMA, martensite reverses back to its original austenite phase. This type of transformation in SMA is known as thermoelastic transformation. The high -temperature parent phase in nonferrous SMA is body-centered cubic(BCC, known as austenite), and on cooling , 24 variants of martensite form, these variants form and grow in self accommodating manner.

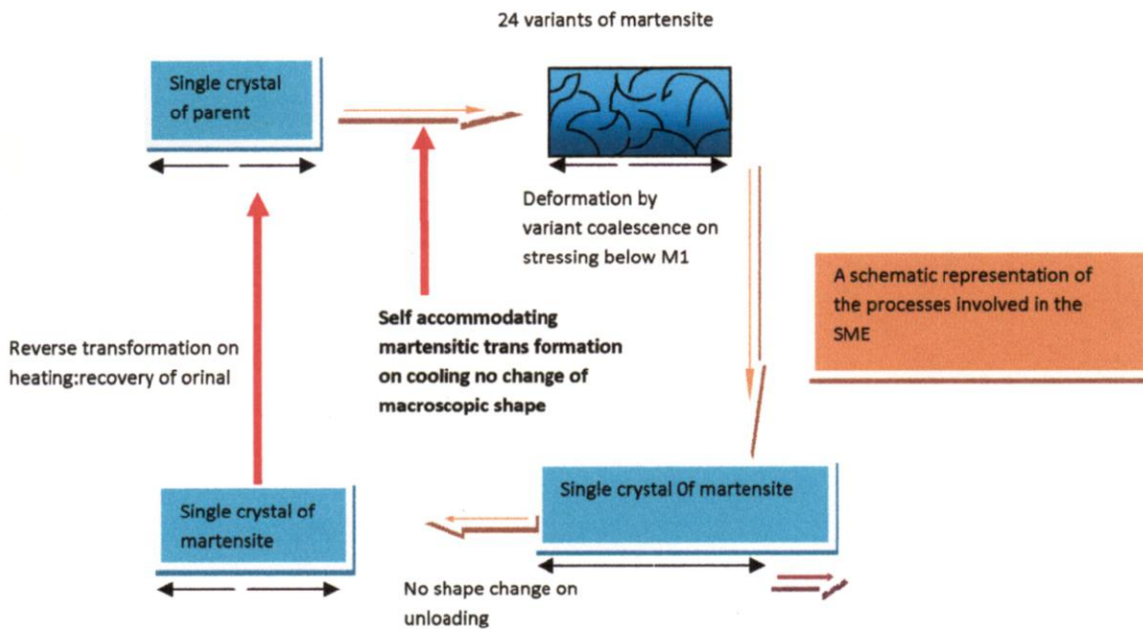


Fig:1.3

One way shape memory

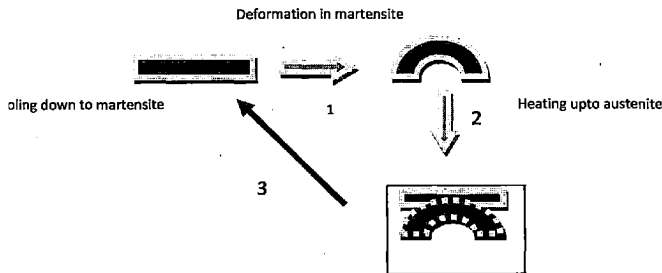
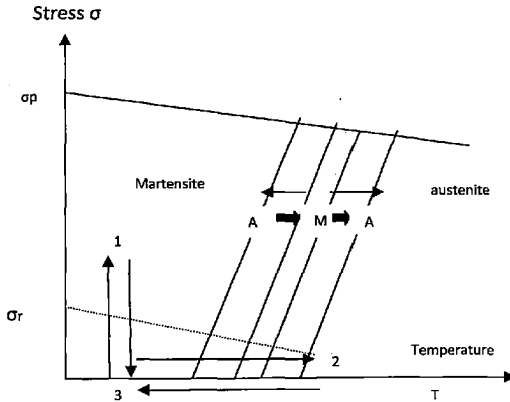


Fig: 1.4

SUPERELASTIC EFFECT: - known also as pseudoelastic, this effect describes material strains that are recovered isothermally to yield a mechanical shape memory behavior. The phenomenon is essentially the same as the thermal SME, although the phase transformation to austenite (A_f) occurs at temperature below the expected operating temperature. If the austenite phase is strained with an applied load, a martensite phase is stress-induced and the twinning process occurs as if the material has been cooled to its martensite temperature. When the applied load is removed, the material inherently prefers the austenite phase at the operating temperature and its strain is instantly recovered.

The stress-strain curve indicates a difference in stress levels during loading and unloading, known as a superelastic stress-strain hysteresis (Fig.4.4) [5].

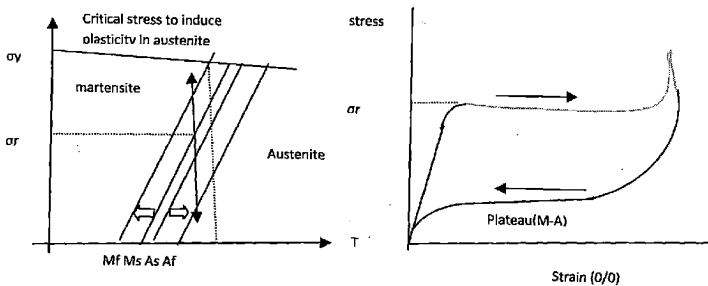


Fig.1.5 an illustration of the superelasticity. The right curve is the superelastic

SMA Systems

Many systems exhibit a martensitic transformation. Generally they are sub divided into ferrous and non ferrous martensites. [21] A classification of the non ferrous martensite was first given by Delsey et al. [21]. While ferrous alloys exhibiting SME were first reviewed by T.Malki and T.Tamura [22].

For all the system, Ni-Ti(X, Y), in which X, Y are elements Ni or Ti. The alloy based on NiTi, popularly known as Nitinol, is the most widely industrially used SMAs alloy [2].the major alloys system is:-

1. Fe based alloys
- 2.Cu-based alloys
- 3.Ni-Ti-based alloys
4. HTSMA
- 5.Other systems [10, 11].

1.4 CHARACTERIZATION TECHNIQUES

There are four major methods of characterizing the transformation in SMAs and a large number of minor methods that are rarely used.

1.The most direct method is by differential scanning calorimeter(DSC) .this technique measures the heat absorbed or given off by a small sample of the material as it is heated and cooled through the transformation-temperature range. The sample can be very small, such as a few mille grams, and because the sample is unstressed this is not a factor in the measurement. The endothermic and exotherm peaks, as the sample absorbs or gives off energy due to the transformation,, and easily measured for the beginning, peak, and end of the phase change in each direction.

2. The second method often used is to measure the resistivity of the sample as it is heated and cooled. The alloys exhibit interesting changes and peaks in the resistivity (up to 20%) over the transformation range.

3. the most direct method of characterizing an alloy mechanically is to prepare an appropriate sample, then apply a constant stress to the sample, and cycle it through the transformation in both directions.

Finally, the stress-strain properties can be measured in a standard tensile test at a number of temperatures across the transformation-temperature range, and from the change in properties the approximate transformation-temperature values can be interpolated.

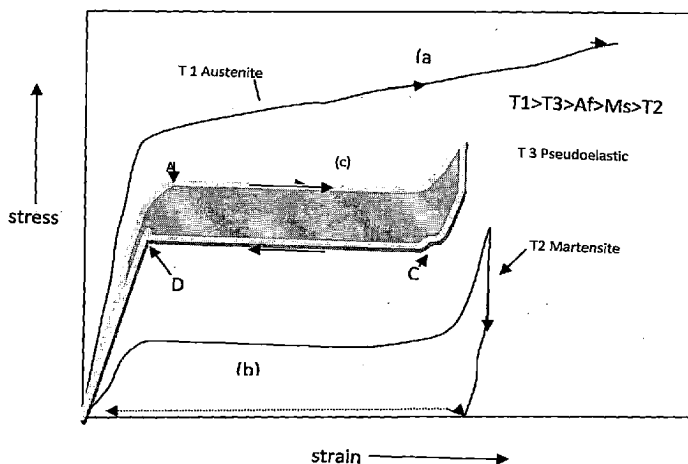


Fig.1.6 Typical stress-strain curves at different temperatures relative to the transformation, showing (a) austenite. (b) Martensite. (c) Pseudoelastic behavior

1.5 FABRICATION TECHNIQUES

There are number of conventional and unconventional techniques of fabrication. Fabrication techniques depend upon type of SMA material and its application. Some of the techniques are as follows:

1. Joining
2. Fusion welding of SMAs
3. Solid state welding of SMAs
4. Alternative processes of joining
5. Transient liquid phase bonding
6. Super plastic forming

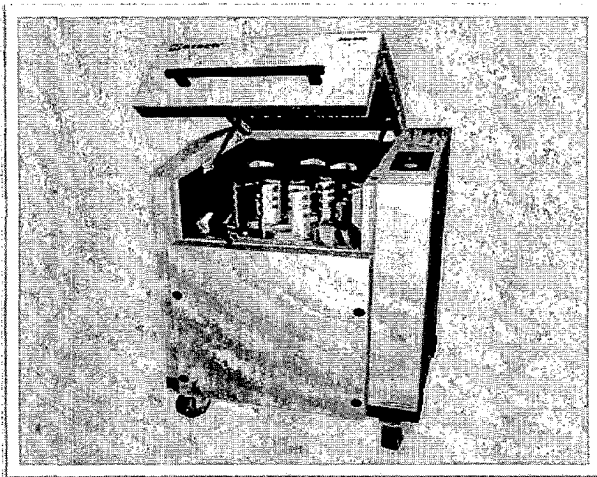
7. Micromachining and fabrication of SMA micro devices
8. Laser machining

1.6 Formation of nano structures by High Energy Ball Milling (HEBM)

Since the 1970s, mechanical attrition (MA) of powder particles as a method for materials synthesis has been developed as an industrial process to easily produce novel alloys and variable phase mixtures. This method can be used to prepare those alloys and composites which cannot be produced by conventional methods of casting and powder metallurgy routes. This method has gained a lot of attention because it is a non equilibrium process resulting in solid- state alloying beyond the equilibrium solubility limit and formation of amorphous or nanostructured materials for a broad range of alloys, intermetallics, ceramics and composites [23, 24]. In the case of mechanical attrition of a binary powder mixture, amorphous phase formation occurs by intermixing of atomic species on an atomic scale, thus driving the crystalline solid solution outside of its stability range against ‘melting’ resulting in solid-state amorphization[25]. This process is considered to be a result of both mechanical alloying [26] and incorporation of lattice defects into the crystal lattice [27].

Mechanical attrition offers interesting options to synthesize nanostructured powders with a number of different types of interface both in terms of structure (crystalline/crystalline, crystalline amorphous) as well as atomic bonding (metal/metal, metal/semiconductor, metal/ceramic, etc.). This brought about exiting possibilities to synthesize advanced materials with particular grain or interphase-boundary design.

A variety of ball mills has been developed for different purposes including tumbler mills, attrition mills, shaker mills, vibratory mills, planetary mills, etc



Retsch PM 400/2 High Energy Planetary Ball Mill set up

Powder with typical particle diameter $\sim 100\mu\text{m}$ is placed together with a number of hardened steel or tungsten carbide (WC) coated balls in a sealed container which is shaken or violently agitated. The most effective ratio of ball to powder masses is between 5 to 10.

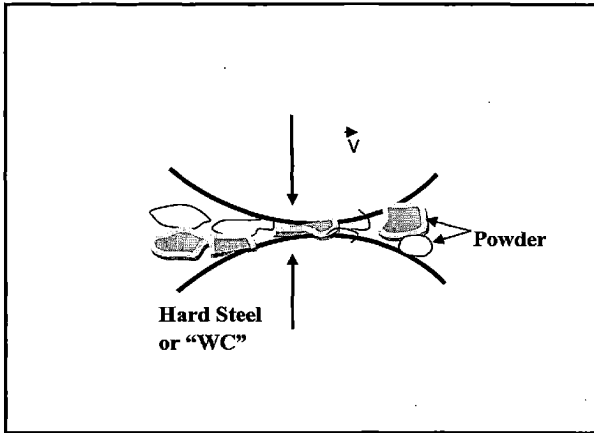


Figure 1.7 Schematic sketch of the process of mechanical attrition of metal powder

Since kinetic energy of the balls is a function of their mass and velocity, dense materials (steel or tungsten carbide) are preferable to ceramic balls. During the continuous severe plastic deformation associated with mechanical attrition, a continuous refinement of the internal structure of the powder particles to nanometer scales occurs during high-energy mechanical attrition. The temperature rise during the process is modest and is estimated to be ~ 100 to 200°C [25].

For all nanocrystalline materials prepared by a variety of different synthesis routes, surface and interface contamination is a major concern.

2.2 Mechanism of Nanostructure Formation

During mechanical attrition metal powder particles subjected to severe plastic deformation from collision with milling balls or tools. Plastic deformation at very high rates ($\sim 10^4$) occurs with the particles and the average grain size can be reduced to a few nanometers after prolonged milling (20 to 80 hrs). This was first investigated in detail for a number of high-melting metals with bcc and hcp crystal structures [28, 29]. Metals with FCC structures are inherently more ductile and often exhibit a stronger tendency to adhere to the container walls and to sinter to larger particles often several millimeters in diameter.

By cold working, the metal is plastically deformed with most of the mechanical energy expended in the deformation process being converted into heat, but the remainder is stored in the metal, thereby raising its internal energy [30]. The x-ray diffraction pattern exhibits an increasing broadening of the crystalline peaks as a function of milling time.

2.3 Mechanism of Grain-Size Reduction

The process leading to the grain size refinement includes three basic stages.

- a. Initially, the deformation is localized in shear bands consisting of an array of dislocations with high density.
- b. At a certain strain level, these dislocations annihilate and recombine as small-angle grain boundaries separating the individual grains. The subgrains formed via this route are already in the nanometer range (~20-30 nm).
- c. The orientation of single-crystalline grains with respect to their neighboring grains becomes completely random. This can be understood in the following way. The yield stress σ required to deform a polycrystalline material by dislocation movement is related to the average grain size d by $\sigma = \sigma_0 + kd^{-1/2}$, where σ_0 and k are constants (Hall-Petch relationship). An extrapolation to nanocrystalline dimensions shows that very high stresses are required to maintain plastic deformation during ball milling

Experimental values for k and σ_0 are typically $k = 0.5 \text{ MN m}^{-3/2}$ and $\sigma_0 = 50 \text{ MPa}$ [31]. For a grain size of 10 nm the minimum stress is of the order of 5 G Pa corresponding to 15% of theoretical shear stress of a hexagonal metal, which sets a limit to a grain-size reduction achieved by plastic deformation during ball milling.

Further energy storage by mechanical deformation is only possible by an alternative mechanism. Grain boundary sliding has been observed in many cases at high temperatures leading to superelastic behavior. Alternatively, grain boundary sliding can also be observed at very small grain size and low temperature by diffusional flow of atoms along the intercrystalline interfaces [32]. This provides a mechanism for the self-organization and rotation of the grains, thus increasing the energy of the grain boundaries proportional to their misorientational angle and excess volume

2.4 Property – Microstructure Relationships

Decreasing the grain size of the material to the nanometer range leads to a drastic increase of the number of grain boundaries reaching typical densities of 10^{19} interfaces per cm^3 . The large concentration of atoms located in the grain boundaries reaching typical boundaries in comparison with the crystalline part scales roughly as the reciprocal grain-size $1/d$

Consequently, due to their excess free volume the grain boundaries in the nanocrystalline cause large differences in the physical properties of nanocrystalline materials if compare with conventional polycrystals. Short-range order typical of an amorphous material is not observed as the characteristic structure of grain boundaries. As such, the grain boundary

structure in these materials must be different from the structure of the single crystal as well as amorphous structure of a glassy material. It turns out that the thermodynamic properties of nanostructured materials produced by MA can be realistically described on the basis of a free volume model for grain boundaries [33]

As a result of cold work energy has been stored in the powder particles. This energy is released during heating to elevated temperatures due to recovery, relaxation process within the boundaries, and recrystallization.

1.7 APPLICATION OF SMAs AND SMART MATERIALS

SMAs have been engineered for applications and devices since the first discovery of the 1930s after the discovery of Nitinol In 1963, since then more than 10000 patents have been issued for applications using SMAs. [35]

Here we would like to discuss some strategically well known SMAs applications and also analysis of smart materials in various applications.

a) Aeronautics/ Aerospace

Due to high power to mass ratio SMA materials gets increasing attention to be used in ideal actuation behavior in zero-gravity conditions.

Designs utilizing these properties replace heavier, more complex conventional devices for weight reduction, design simplicity and reliability.

b) Smart Airplane Wings

Composite structures embedded with SMA wires can be used to change the shape of an airplane wing. The embedded wire is activated to constrict and improve vibration characteristics of the wing. It can be heated to change their effective modulus to reduce vibration, or activated to alter the shape of the wing for optimal aerodynamics. All of these properties can be used to produce an adaptive airplane wing, altering as environmental conditions change to improve efficiency and noise reduction

c) Self-erectable antennas

A prototype space antenna was constructed by Goodyear Aerospace Corporation. Designed to fold compactly at room temperature. The device would unfold to a large, extended antenna shape when heated with solar energy. [34, 36]

d) Space system vibration damper

Comprised of composite materials using restrained, embedded SMA wire or ribbons, vibration dampers can reduce unwanted motion in various space systems. A sensor detects

vibration in the system and sends a signal to activate the embedded composite, which then alters the structural dynamics to damp or cancel the existing vibration.[37]

e) Consumer products

SMA devices and components have been used in high-volume consumer products for more than 25 years. Although many consumers who use these products are unaware of their SMA components, there is growing public awareness of SMAs due to recently marketed items that advertise their merits.

- i. **Flexion Optical Frames:** - superelastic eyeglass frames are one of the most widely known uses for SMAs. The components of eyeglass frames that are most susceptible to bending, **the bridge and temples** are wire forms of Ni-Ti, the remainder of frame is made of conventional materials for cost saving.
- ii. **Greenhouse Window opener:-** now days it has become a fashion to equip these windows in modern commercial buildings for automatic temperature control. The opener is a spring- loaded hinge that has a Cu-Zn-Al shape memory spring and a conventional metal biasing spring. The SMA spring is compressed by the metal biasing spring at temperature below 18°C , and the window is closed. The SMA spring activates around 25°C , overcome the force of bias spring, and open the window.
- iii. **Robotic Doll:** - SMA actuator wires were designed to move the arms and legs of a doll to display human characteristics. The application is technically feasible and prototypes were successful; however, the power requirements to activate the wires were too great. It limits the market acceptance of the product.

f) Medical

The medical industry is rapidly accepting the use of SMAs in wide variety of applications. Ni-Ti has been adopted by the industry for its ability. It is excellently biocompatible and corrosion resistant; I-Ti has been used in many successful medical devices and is now widely accepted throughout the medical industry .some popular one are-

- i. Orthodontic Dental Arch Wires
- ii. Mite Homer Mammal
- iii. Guide wire Cores
- iv. **Stents:** - SMA Stents are becoming increasingly popular in the medical industry. These structural, cylindrical components, designed to prop open and support human blood- vessels wall, ducts, and other human passage-ways, are implanted to prevent collapse or blockage and to path lesions. Stents currently on the market and in development use various functional properties of SMAs: these are
 - ✦ Superelasticity of austenite
 - ✦ Thermal shape memory
 - ✦ Low effective modulus of martensite
 - ✦ Many of these SMA Stents use a combination of superelastic and shape memory properties.

For example stent may be chilled in ice water for transformation to martensite, compressed in martensitic state, covered in protective sheath for a minimal profile, and then delivered into the body through a small portal. When in place, sheath is removed, and stent warms to body temperature to recover its original shape

g) Power Generation System

The Central Research Institute of the Electric Power Industry in Tokyo [38] has been engaged in research to develop a power generation system using a Ni-Ti based SMA with objective of effective utilization of low- temperature exhaust heat for power generation. The system does not utilize heat intact but rather convert's heat into motive power via an SMA engine, stores the energy and revolve a generator whenever necessary. When attempting to utilize the heat generated by power plants and waste incineration plants, the heat lost will be extremely large when transporting the heat over long distances, so heat utilization will naturally be restricted to nearby areas. Therefore, an attempt was made to ultimately convert this heat into electricity, by the use of an SMA that can be activated at low temp. And with small temp. differences. Using this alloy as the energy conversion element will enable motive power to be obtained from untapped low-temperature energy resources.

Shape memory alloys elongation and contraction

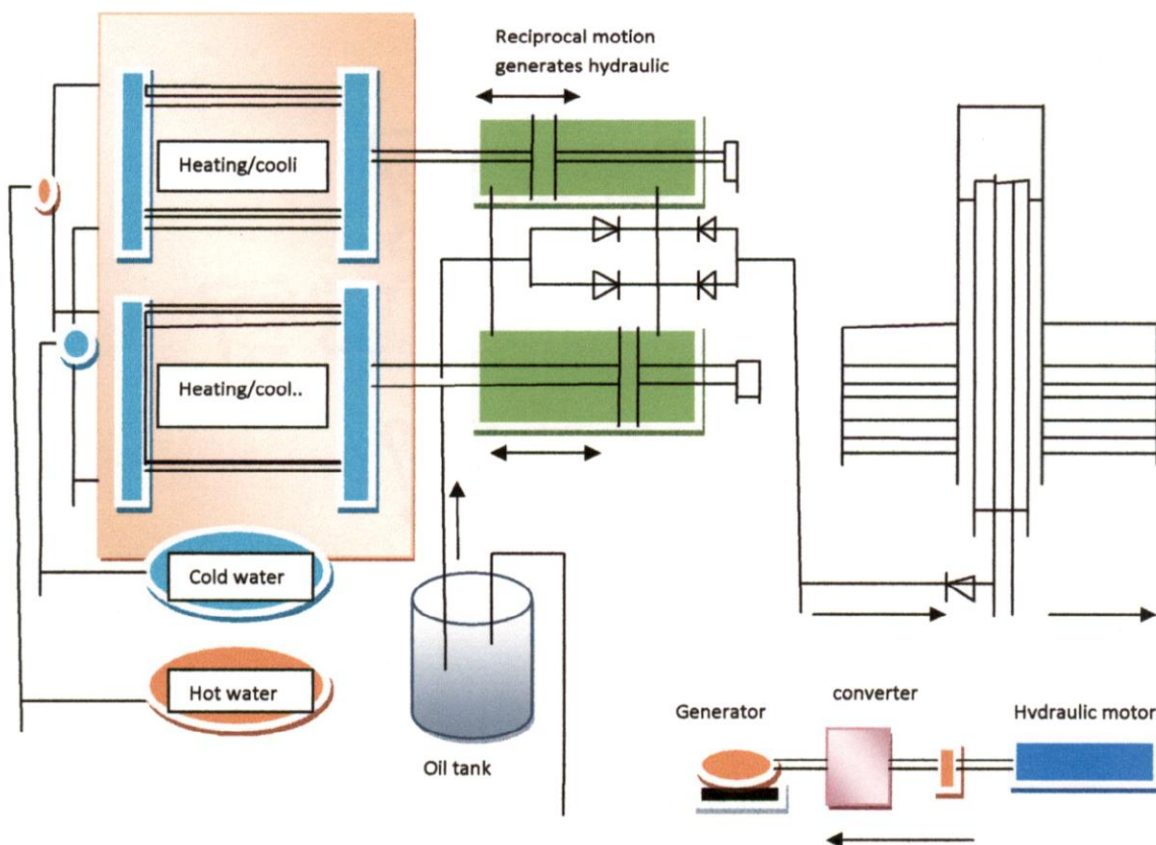


Fig:1.8 Mechanism of engine and power generation using SMA [155]

Chapter: 2 Literature Survey

Li Lu and M O Lai Department of Mechanical and Production Engineering, National University of Singapore, in his paper of “formation of new materials in the solid state by mechanical alloying” in 1995 have observed Several key factors, which control the formation of new alloys. These factors are, activation energy, which is related to the formation of defects during collision of powder particles and sliding between those particles; temperature which is associated with plastic deformation of powder particles; and crystalline size, which is related to the formation of nanometer crystalline during mechanical alloying. It is found that the diffusion process during mechanical alloying is controlled by both mechanical and thermal energy. The activation energy can be lowered by introducing defects, which in turn results in increase diffusivity. By reducing grain size, effective diffusivity can be increased significantly. Grain boundary and free surface diffusion are found to prevail to enable diffusion to proceed at relatively low temperature.

J.X Zhang, Y.X.Liu, W, Cai, L.C.Zhao, in 1997 in his work of “*The mechanism of two way shape memory effect in a Cu-Zn-Al alloy*” Authors presented in paper, TWSME can be achieved by suitable Thermomechanical training and processing. Sample studied by authors was polycrystalline shape memory alloy Cu_{20.4}Zn_{5.6}Al (wt %) was melted in induction furnace. Ingot was homogenized at 850°C for 12 hrs, rolled into the sheets, and then spark machined into strips of 200x4x1mm. the specimen were then betatized at 850°C at 10 min, quenched into boiling water, aged at 100°C for 20 min, and then air cooled at room temperature. Transformation temperature were measured by DSC are M_s=78°C, M_f=40°C, A_s=50°C, A_f=86°C.

In this work it can be concluded that mechanism of two-way shape memory effect are different due to different training routines. The combined SIM and SME training mainly results in suitable dislocation array.

M. Franz, E Hornboen, in his paper “*Martensitic transformation of a Cu-Zn-Al shape memory alloy strengthened by hot rolling*” in 1998, have emphasized that lattice defects were introduced into stable austenite (β) of a Cu₂₇Zn₂₇Al₄ alloy by a hot rolling and quenching process (Ausforming, AF). The amount of deformation was varied between zero and 1.54, the AF temperature T (AF) between 800 & 650°C. At T (AF) < 700°C the alloying forms a mixture of (α + β) phase and is renders untransferable, while the other ausforming treatments do not reduce transformability. They lower the temperature range of martensitic transformation cycles and improve considerably the conventional strength properties. The interpretation of these results is based on the microstructure, especially the defect structure in austenite.

On the selection of shape memory alloys for actuators, W. Huang. School of Mechanical and Production Engineering, Nanyang Technological University in 2001, presented a series of charts for selection of SMA_s for actuators in particular, at the pre-design stage. In this paper emphasis is given on three most popular polycrystalline SMA_s, namely NiTi, Cu Zn Al and Cu Ni Al.

The discussion is purely based on material properties reported in the literature. There are three basic types of SMA actuators.

- One way actuators
- Biased actuators
- Two way actuators

SMA's may be heated up by three methods

- a. Passing electrical current (small dia)
- b. Passing electrical current through high resistance wire
- c. By hot air/water or exposing to thermal radiation.

Material selection is based on various parameters these are.

- i. Transformation temperature & hysteresis
- ii. Output work
- iii. Actuation stress and strain, if light weight actuator is a goal, instead of actuation stress (= stress/density) should be as high as possible
- iv. Heating and cooling speed
- v. Energy efficiency (higher energy efficiency is critical). Output work per kg/min. input power per kg
- vi. Cost
- vii. Damping (high damping capacity is an attractive property of SMA's).

Based on comparative parameters above mentioned Ni Ti is the overall winner with respect to most of the thermo-mechanical related performances. When material cost is taken into consideration, Cu Zn Al should be the first choice, followed by Cu Zn Ni. Cu Zn Al is the most suitable choice for damping related actuators.

Hyoun woo Kim, School of Material Science and Engineering, Inha University, in his work "study of two-way shape memory effect in Cu Zn Al alloy by Thermomechanical cycling method".in2003,

Has given emphasis on Cu based shape memory alloy, due to its easy fabrication, excellent conductivity, both electrical and thermal. Author has tried to show two way shape memory effect by bending alloy samples around cylindrical shaped structures and employing a constrained heating cooling techniques.

Bending profiles of strips are not actual rather artificial, this creates doubt over proclaimed results.

However author selected two samples of CuZnAl variation in composition for comparative analysis. Alloys were prepared in induction furnace and subsequently forged and hot rolled. Rectangular specimens with 170mmx12mmx2.2mm were machined. Specimens were beta-tized at 800 °C for 30 min. and quenched in 25°C of water. Transformation temperature were calculated by measuring the electrical resistance of the samples indicating Ms =20°C, As =30°C and Af= 61°C, Mf =0°C for 70.3 Cu 24.1 Zn-5.6 Al alloy. For second sample Ms = -70°C, Mf =-100°C, As = -4.8°C and Af= -20°C for 65.6Cu-33.1Zn-1.3Al alloy.

As results shows TWME in two samples was induced by a training method with cycles of constrained heating/cooling. The mechanical strength of the alloys was achieved by bending around a cylindrical mould in liquid nitrogen. The strength of TWME tends to increase with increasing number of Thermomechanical cycles.

The constrained heating temperature also affects TWME significantly. Presence of β -phase and thus martensitic structure is a crucial factor in generating TWME. After Thermomechanical cycling treatment, it is observed that new martensitic structure inclined with some angle to existing martensitic structure.

L. Hopulele, S. Israti, S. Stancu, G H Caluguru. Technical University "Gh Asachi" Iassy, in their work, "Comparative study of certain Cu-Zn-Al type alloys concerning their superelastic behavior and shape memory".

Authors have taken 11 samples with composition Cu-(14-25) wt% Zn-(3-6.5)wt% Al out of which three were selected for final study. Three samples named as A, B and C alloys presented similar value of the tensile strength (200-220) Newton/mm². Each sample stressed at 20 °C loading unloading cycles.

Samples from the alloy have been subjected to dilatometric analysis within the temp.range 20-140 °C.

As for as sample C is concerned , light increases by 0.19% wt% Zn concentration and by 0.28%wt of Al concentration as compared to B alloy lead to the drift of the critical transition points within the positive temperature range, and therefore to the occurrence of shape memory effect.

After plastic processing by hot hammer forging at t=820°C and water hardening treatment the C alloy has registered an improvements of its tensile strength between 260-280 N/mm²

We can conclude that the studied Cu-Zn-Al alloys, a narrow range modification of the chemical composition does not result in important alteration of the unit tensile loading but it leads to significant differences with respect to the pseudoelastic properties and shape memory effect. Chemical composition has a deciding influence on the position of the critical temperatures and shape memory effect. This study is based on sample prepared by conventional (casting) method; it does not elaborate features of Nano Structure in Shape Memory Effect.

Z. Li , S. Gong, M.P Wang , School of Materials Science and Engineering central South University, Changsha, 2006 in their paper, "Macroscopic shape change of Cu13 Zn15Al

Shape Memory Alloy on successive heating”, Authors have related substructural anisotropy in the parent phase is responsible for (TWSME). This anisotropy is due to array of dislocations created by a special thermo-mechanical cycling, through the martensitic transformation, either by stress cycling at a fixed temperature or by temperature cycling at a fixed stress.

Transformation temperatures are measured by electrical resistivity measurement.

The shape change and transformation process of the Cu-13Zn-15Al (at %) alloy on successive heating and cooling has been investigated by electrical resistivity measurement, optical metallographic observations and X ray diffraction. It can be concluded that the martensite stabilization process in Cu-13Zn-15Al alloy not possesses a martensitic nature but also possesses diffusion- control nature. The martensite stabilization is accompanied by:

- a. As increasing
- b. The abnormal surface re-relief phenomenon emerging
- c. The reverse shape memory effect occurring
- d. The monoclinic angle β of the martensite tending to 90°

As the heating temperature is below 320°C , the FR SME in the Cu-13Zn-15Al alloy occurs due to martensitic nature transformation in the martensitic stabilization process, between 320 & 400°C , the FSME in the Cu-13Zn-15Al alloy exists due to the reverse transformation of the stabilized martensite.

As the heating temperature is higher than 450°C and then air cooling, the SRSME in the Cu-13Zn-15Al alloy occurs, which attributes to the growth of an asymmetric martensitic phase due to restraint of the α - phase distributed along the boundary of the new formed martensitic variants.

S.K Vajpayee R.K Dubey. M.Sharma, in 2009 Studies on the “mechanism of the structural evaluation in Cu-Al-Ni elemental powder mixture during high energy ball milling”

They discuss about phase and microstructural evolution during alloying of 82Cu-14Al-4Ni powder mixture.

X-ray diffraction pattern shows that relative intensity of the Al peaks decreased with milling time and Al peaks almost disappear after 32 hr milling time. The gradual decrease in the Al G peak intensity indicated dissolution of Al in the Cu matrix with increasing milling time. A slight shifting of Cu peaks towards lower angles, with increasing milling time is further confirmation of diffusion of Al and Ni in Cu matrix to form the solid solution. The lattice parameter as calculated using Xrd data of resulting solid solution ($a=0.36061\text{nm}$) was found to be close to that of the starting Cu powder ($a=0.35957\text{nm}$).

It is concluded that a disoriented single phase solid solution was formed after 48 hr of milling of the elemental Cu, Al, Ni powder.

Though paper is related to shape memory alloy but it skip on Shape Memory Effect. it is focused on effect of milling hours on physio-morphological changes occurs and nanocrystallization.

G Betolino, A Gruttadauria, P Arneodo Larochetta, E M Castrodeza, A Baruj, H. E Troiani, in their work of, "Cyclic pseudo-elastic behavior and energy dissipation in as-cast Cu-Zn-Al foam of different densities". Presents the mechanical properties of pseudoelastic Cu-Zn-Al foams, of different densities were cycled in compression. The retained/dissipated energy by the material, i.e. the area of the compression cycle, as a function of the material density. The frequency and strain amplitude usual parameters that may influence the damping properties are studied by evaluating the dissipated energy and the specific damping capacity. Samples cyclically tested under constrained compression conditions show a remarkable mechanical stability and reproducibility. The material does not appreciably degrade after 10000 compression cycles at room temperature. It can be concluded that material does not need any Thermomechanical processing or training treatment in order to present the mechanical properties

Chapter: 3 Experimental Methods

In this chapter I will like do discuss experimental methods and about related instruments used in conduction of experiments.

3.1 X-Ray Diffraction

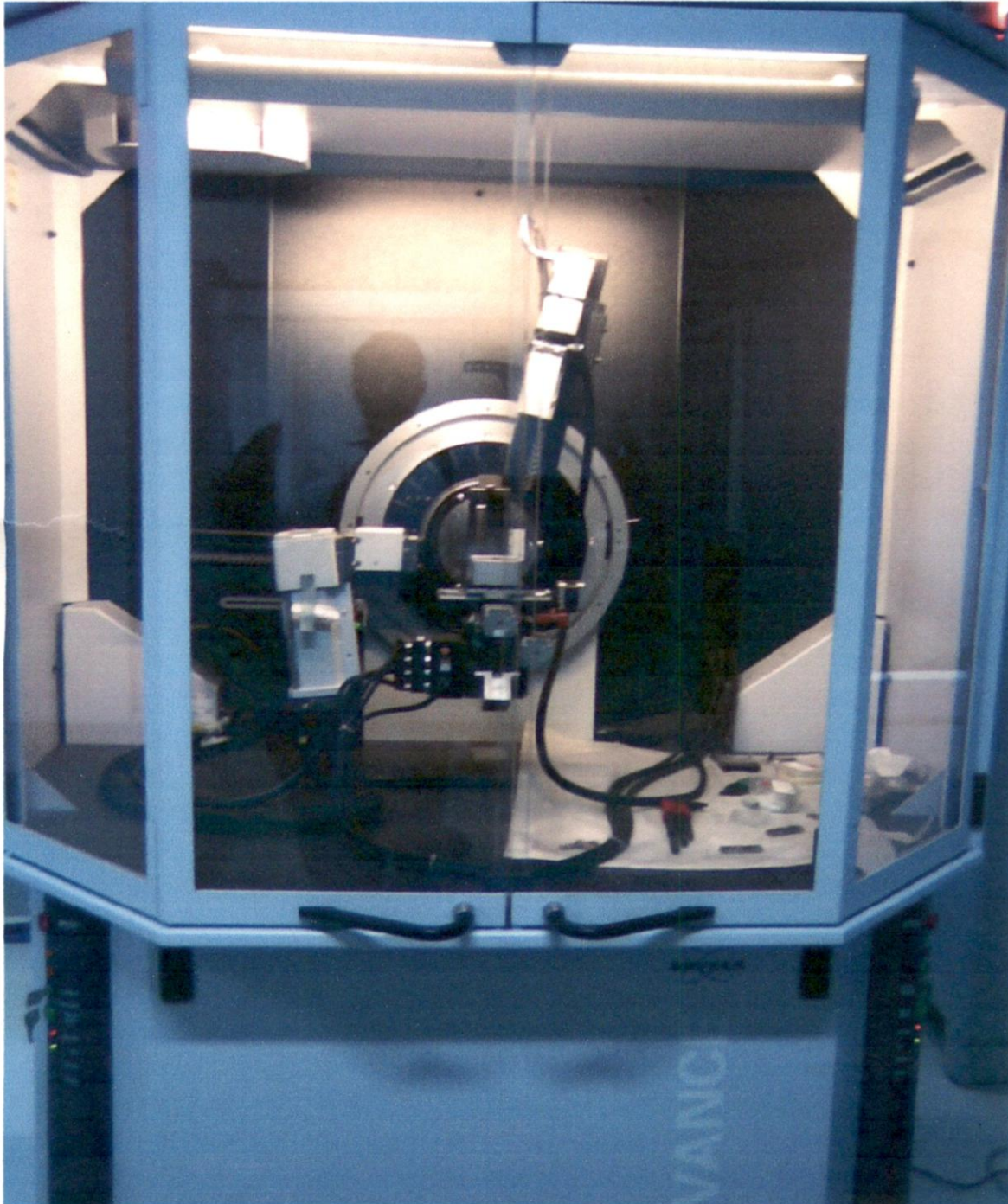


Fig: 3.1 view of Bruker D-8 X-RD machine at I.I.C Roorkee.

Bruker D-8 Specification

Target Facility Cu, Mo, Fe, working voltage= 10-100Kv, Tube Current= 40-80 mA

Goniometer Scanning speed= 0°-150°

In our project work X-ray diffraction is carried out using X-ray diffractor (Bruker D-8 Advanced Germany) with Cu K α radiation at 40 kV and 20 mA, with scanning speed of 1° per min from 20°-90°. Cu K α radiation of $\lambda = 1.5418 \text{ \AA}$.

Milled samples were collected at different intervals for X-RD analysis. Purpose of XRD analysis is to find out widening of peak of highest intensity and also find out relative intensities of different peaks with increase in milling time. Scherer formula was the basis to calculate widening of peak.

a. Grain Size Analysis: Scherer's Formula

$$B = 0.9\lambda / t \cos\theta$$

B= Broadening of diffraction line measured at half its max. Intensity

t=diameter of the crystal particle

λ =wavelength of X-ray K α line for Cu K α $\lambda = 1.54 \text{ \AA}$

b. Calculation of Lattice Strain:

According to law of X-ray diffraction pattern

$$2d \sin\theta = n\lambda$$

$$2(d+\Delta d)\sin(\theta + \Delta\theta) = n\lambda$$

$$2(d+\Delta d)(\sin\theta\cos\Delta\theta + \cos\theta\sin\Delta\theta) = n\lambda$$

$$2d\sin\theta\cos\Delta\theta + 2d\cos\theta\sin\Delta\theta + 2\Delta d\cos\theta\sin\Delta\theta + 2\Delta d\sin\theta\cos\Delta\theta = n\lambda$$

$$2d\sin\theta + 2d\cos\theta\Delta\theta + 2\Delta d\Delta\theta\cos\theta + 2\Delta d\sin\theta = n\lambda$$

$$2d\sin\theta = n\lambda, \quad \text{and} \quad 2\Delta d\Delta\theta\cos\theta = 0, \text{ (equivalent to zero)}$$

$$2d\cos\theta\Delta\theta + 2\Delta d\sin\theta = 0$$

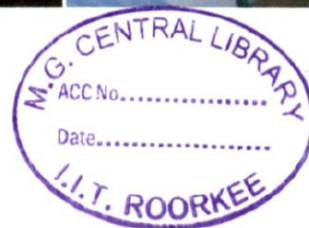
$$\Delta d/d = - \Delta\theta/\tan\theta$$

Here $\Delta d/d$ is lattice strain and $\Delta\theta$ is angular width at half maxima, using this equation we can calculate lattice strains with respect to milling hours of material.

3.2 SEM (Scanning Electron Microscopy)



Fig: 3.2 SEM Systems at IIC Roorkee



Specification of the system:

How it works: it employs a beam of electrons directed at the specimen. SEM primarily to study the surface, or near surface, structure of bulk specimens.

The electron source (or gun) is usually of the tungsten filament thermionic emission type, although field emission gun (FEG) source are increasingly being used for higher resolution. The electrons are accelerated to an energy which is usually between 1 keV and 30 keV, which is considerably lower than the energies typical of the TEM (100-300keV). The two or three condenser lenses then demagnify the electron beam until, as it hits the specimen, it may have a dia meter of only 2-10 nm.

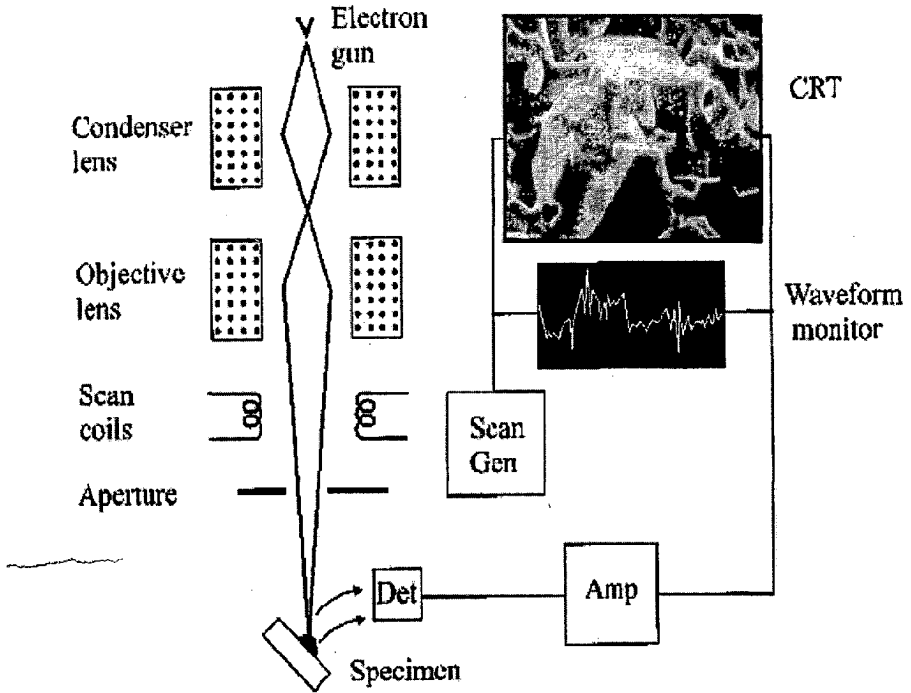


Fig: 3.3 Schematic diagrams showing the main components of a scanning electron microscope.

The mechanism by which the image is magnified is extremely simple and involves no lens at all. The raster scanned by the electron beam on the specimen is made smaller than the raster displayed on the CRT. The linear magnification is then the side length of the CRT (L) divided by the side length (l) of the raster on the specimen.

For example, if the electron beam is made to scan a raster $10\mu\text{m} \times 10\mu\text{m}$ on the specimen, and the image is displayed on a CRT screen is $100\text{mm} \times 100\text{mm}$, the linear magnification will be $10000\times$. All scanning electron microscopes normally have facilities for detecting secondary electrons and back scattered electrons.

3.3 FE-SEM & EDAX



Fig: 3.4 FE-SEM EDAX SYSTEM AT I.L.C Roorkee

A. Specification of the system

Specification of Microscope: Instrument QUANTUM, 200 FEG

Marketed by FEI Netherlands, High Voltage 200kV.

B. Working principle

Under high vacuum less than 10^{-7} Pascal electron generated by a Field Emission Source are accelerated in a field gradient. The beam passes through Electromagnetic lenses, focusing into the specimen. As result of this bombardment different types of electrons are emitted from the specimen. A detector catches the secondary electrons and an image of the sample surface is constructed by comparing the intensity of these secondary electrons to the scanning primary electron beam. Finally the image is displayed on a monitor.

C. Field Emission Source The function of electron gun is to produce a large and stable current in a small beam. There are two classes of emission sources; thermionic emitter and field emitter. Emitter type is the main difference between the (SEM) and (FESEM).

Thermionic Emitters use electrical current to heat up a filament, the two most common materials used for filaments are Tungsten (W) and Lanthanum Hexaboride (La B6).

Thermionic sources have relatively low brightness, evaporation of cathode material and thermal-drift during operation. A Field Emission Source also called a cold cathode field emitter, does not heat the filament. The emission is reached by placing the filament in a huge electrical potential gradient.

FESEM uses Field Emission Source producing a clear image, less electrostatic distortion and spatial resolution less than 2nm (3 to 6 times better than SEM).

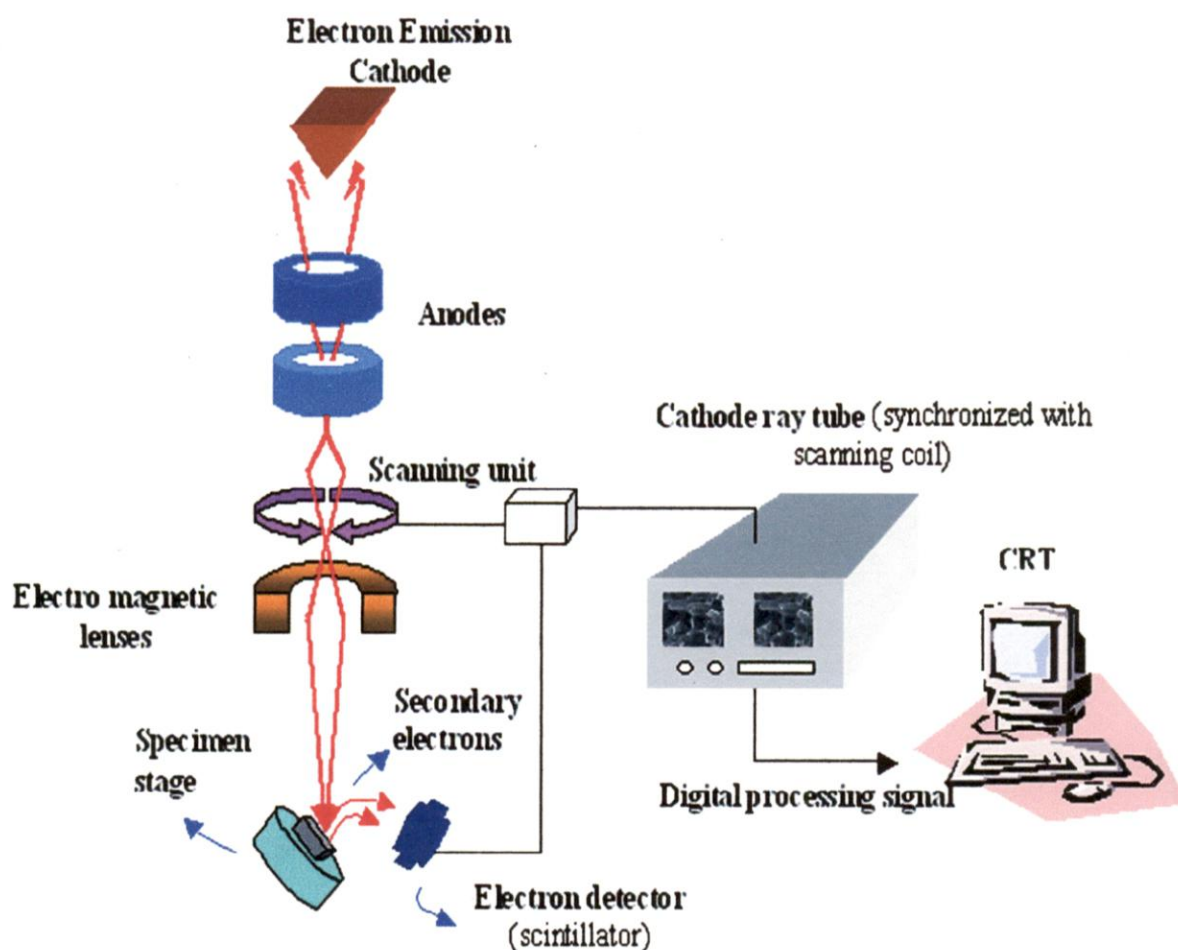


Fig: 3.5 FESEM Schematic Working Principles.

D. EDAX (Electron Dispersive X-Ray Spectroscopy Analysis)

EDX is a technique used in conjunction with chemical micro-analysis by scanning electron microscopy (SEM). EDX technique detects X-rays emitted from the sample during bombardment by an electron beam to characterize the elemental composition of the volume analyzed. When the sample is bombarded by the electron beam SEM, the electrons are ejected from atoms comprising the sample surface. The resulting electron vacancy is filled by

electron from a higher state, and an X-ray is emitted to balance the energy difference between the two states of electrons. The x-ray energy is characteristic of the element from which it was issued.

EDS x-ray detector measures the relative abundance of x-ray against their energy. The detector is typically a lithium silicon solid state device. When an incident x-ray hits the detector, which creates a pulse of charge that is proportional to the energy of x-ray. The pulse charge is converted to a pulse voltage (which is proportional to the energy of x-ray) by a charge sensitive preamplifier. The energy, as determined by measuring the voltage per incident x-ray is sent to a computer for display and further data evaluation. The spectrum of x-ray energy versus count is evaluated to determine the elemental composition of sample volume.

Information Analysis:

A. Qualitative Analysis: the sample volume from x-ray energy spectrum EDS are compared with known characteristic x-ray energy values to determine the presence of an element in the sample. Elements with atomic numbers ranging from beryllium to uranium can be detected. The lower limit of detection range from about 0.1% to an atom of a few percentage points, depending on the element and sample matrix.

B.The Quantitative Analysis: Quantitative results can be obtained from the count on the x-ray energy levels characteristic for components of the sample.

C.Elemental Mapping: Characteristic x-ray intensity is measured relative to the lateral position on the sample. Variation in the intensity of x-ray in any characteristic value indicates the relative concentration of energy for the item applicable through the area.

C.Typical Application

- ✦ Analysis of foreign material
- ✦ Evaluation of corrosion
- ✦ Analysis of composition of coatings.
- ✦ The rapid identification of the material alloy.
- ✦ Analysis of material small items
- ✦ Phase identification and determination.

3.4 Pellet making, Sintering (Heat Treatment in controlled Environment to prevent oxidation)

Pellets of milled powder were prepared using hydraulic press at Nanotechnology lab. Max applied load in this press is 15 Ton. Dia of Die and Punch is 12mm. purpose of pellet formation is to-check materials micro hardness. Load was applied manually by hand lever.

For Cu Zn Al powder no binder required. For making pellet of 12 mm dia and 5mm thickness applied load needed is 5 ton.

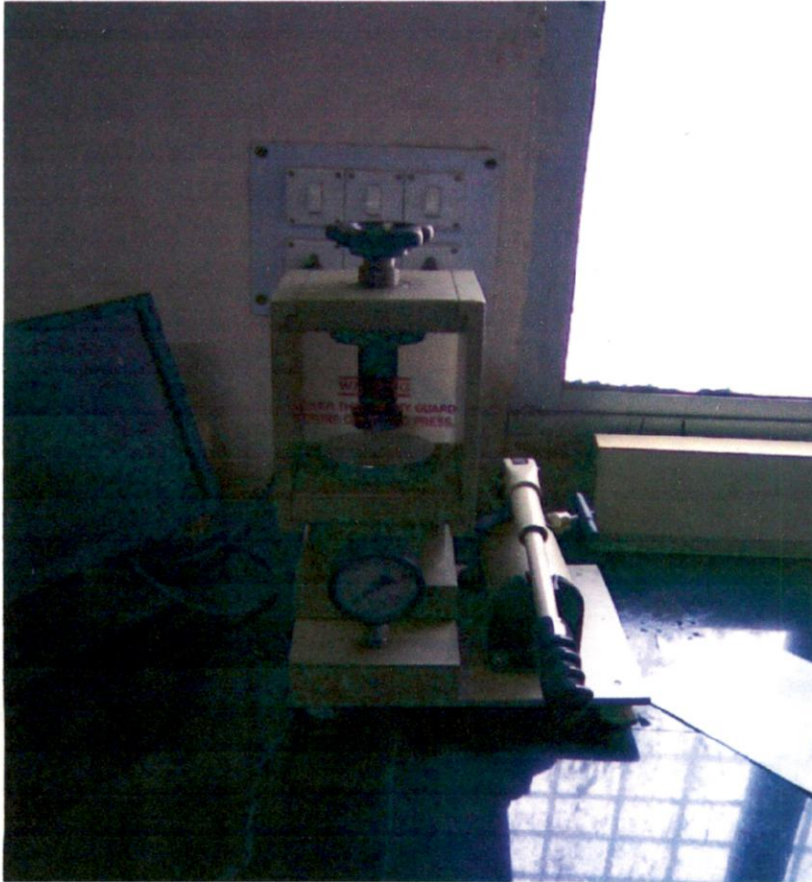


Fig: 3.6 manually operated hydraulic press at Nanotech lab I.I.T Roorkee.

A. Green Pellets prepared in hydraulic press.

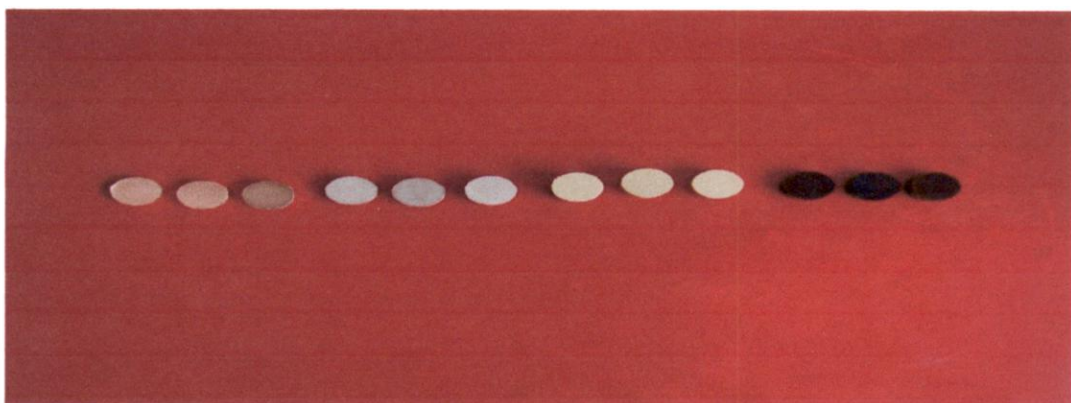


Fig:3.7 Green pellets of 12 mm dia from left to right(three in group) as mixed, 2hr milled, 20 hr milled and 48 hr milled powder.

B.Sintered pellets heat treated at 500°C in presence of hydrogen gas flow in order to prevent oxidation of material for 1 hr.

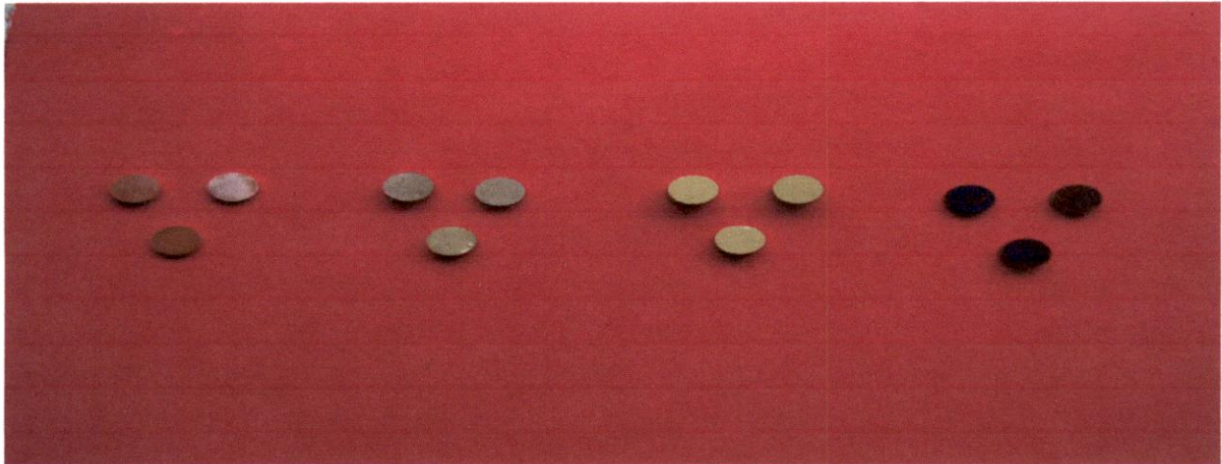


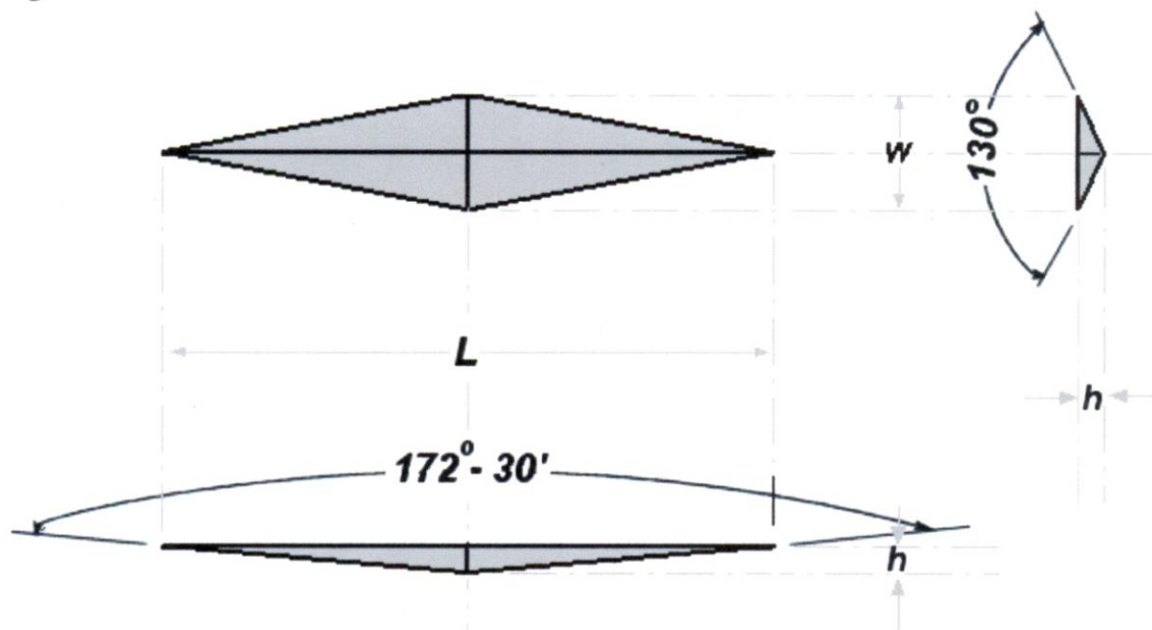
Fig: 3.8 from left to right (Three in group) as mixed, 2hr, 20hr, and 48hr milled powder pellets.

3.5 Microhardness Testing of Pellets

The term micro hardness test usually refers to static indentations made with loads not exceeding 1 kgf. The indenter is either vickers diamond pyramid or the knoop elongated diamond pyramid. The procedure for testing is very similar to that of the vickers hardness test, except that it is done on a microscopic scale with higher precision instruments. The surface being tested generally requires a metallographic finish. The smaller the load used, the higher the surface finish is required. Precision microscopes are used to measure the indentations these usually have a magnification 500X and measure to an accuracy of $\pm 0.5 \mu\text{m}$.

Fig:

3.9



The Knoop hardness number KHN is the ratio of the load applied to indenter, P (kgf) to the unrecovered projected area A (mm²).

$$KHN = F/A = P/CL^2 \quad \text{where}$$

F = applied load in kgf

A = the unrecovered projected area of the indentation in mm².

L = measured length of long diagonal of indentation in mm.

C = 0.07028 constant of indenter relating projected area of the indentation to the square of the length of the long diagonal.

The Knoop indenter is a diamond ground to pyramidal form that produces a diamond shaped indentation having approximate ratio between long and short diagonal of 7:1. The depth of indentation is about 1/30 of its length.

3.6 Hot Forging:

After sintering pellets in presence of hydrogen gas flow inside the specially designed steel tube, for about 1 hr. sintering operation was performed to normalization and stress relieving. Some minor grain boundary readjustment may takes place, but there is no any significant change in internal structure and mechanical properties takes place.

In hot forging pellets heated up to below melting point about 800°C (red hot), taken immediately on the platform of forging machine and forged.

3.7 Hot Rolling:

Hot rolling operation was performed to convert pellet into thin sheet or strip. Pellets were heated in furnace red hot and immediately rolled. Number of passes required to roll the pellet to get desired thickness

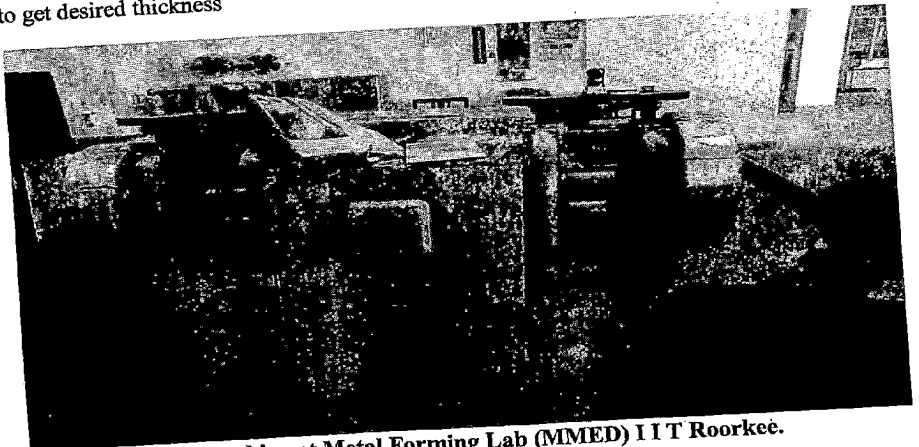


Fig: 3.10 Rolling machine at Metal Forming Lab (MMED) IIT Roorkee.

3.8 Optical Metallography:

Metallography is the study of metals optical and electron microscopes. Structures which are coarse enough to be discernible by the naked eye or under low magnifications are termed macrostructures.

Those which require high magnification to be visible are termed microstructures. Microscopes are required for the examination of the microstructures of the metals.

Optical microscopes are used for resolutions down to roughly the wavelength of the light (about half micron).

Microscope can give information concerning material composition, previous treatment and properties. Particular features of interest are.

- I. Grain size
- II. Phase present
- III. Chemical homogeneity
- IV. Distribution of phases
- V. Elongated structures formed by plastic deformation.

Specimen prepared for optical microscopy:

The preparation of a specimen to reveal its microstructure involves.

- + Cutting the section by diamond cutter machine
- + Mounting in resin if sample is small
- + Coarse grinding
- + Grinding on progressively finer emery paper
- + Polishing using alumina powder or diamond paste on rotating wheel
- + Etching on dilute acid Washing in alcohol & drying

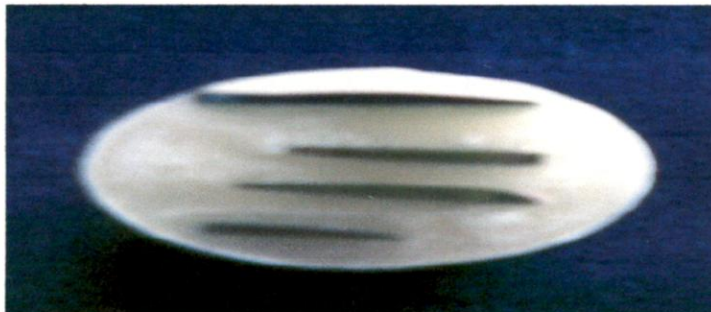


Fig: 3.11 mounted samples in order (as mixed, 2, 20, 48 hr milled hot forged, from bottom to top)

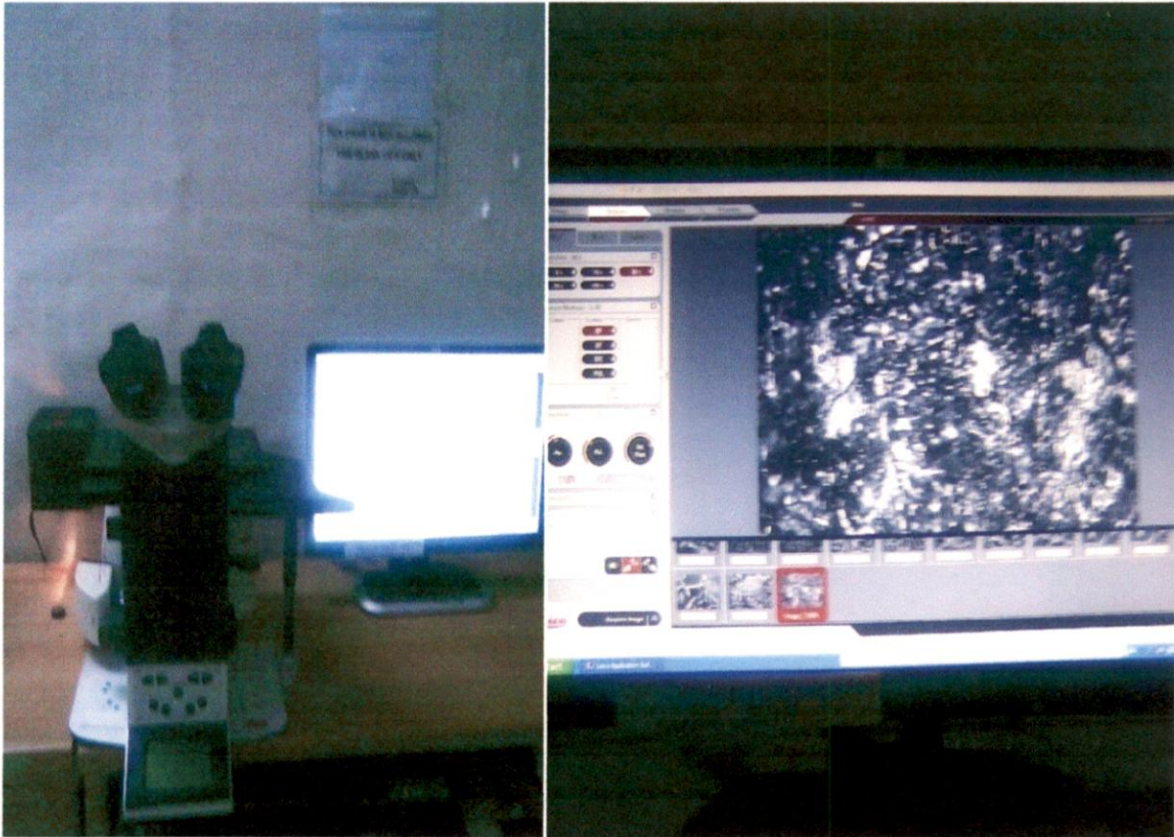
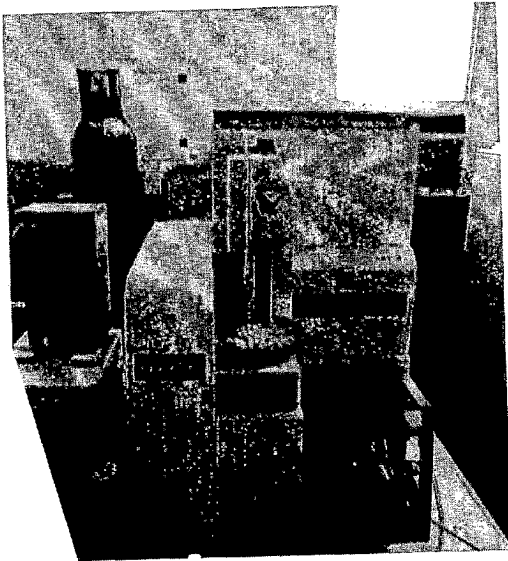


Fig: 3.12 Optical Microscope (Leika) System at Metallography Lab MMED I I T Roorkee. Magnification (50X to 1000X).

3.9 DTA/DSC DTG Analysis of the sample



3 Perkin Elmer Thermal Analyzer (Pyris Diamond) at I I C Roorkee.

6300, Max Temp 1500°C, inert gas H₂, N₂.

Thermogravimetric Analysis (TGA)/Differential Thermal Analysis (DTA)

Thermogravimetric analysis (TGA) is a thermal analysis technique which measures weight change in a material as a function of temperature and time, in a controlled atmosphere. This can be very useful to investigate the thermal stability of a material, or its behavior in different atmospheres (e.g. inert or oxidizing). It is suitable for use on solid materials, including organic or inorganic materials.

Differential thermal analysis (DTA) is a calorimetric technique, recording the temperature change associated with thermal transitions in a material. This enables phase transitions (e.g. melting point, glass transition temperature, crystallization etc.).

Chapter: 4 Results and Discussion

Fig: 4.1 Cu Powder XRD

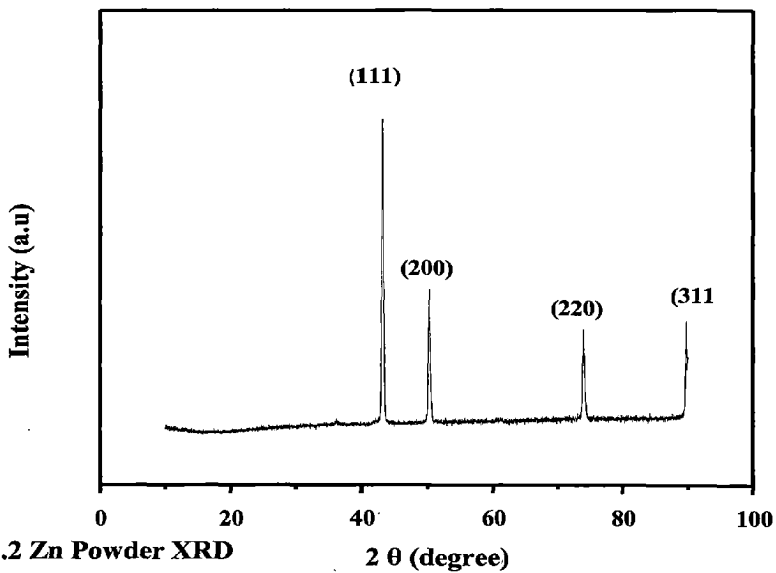
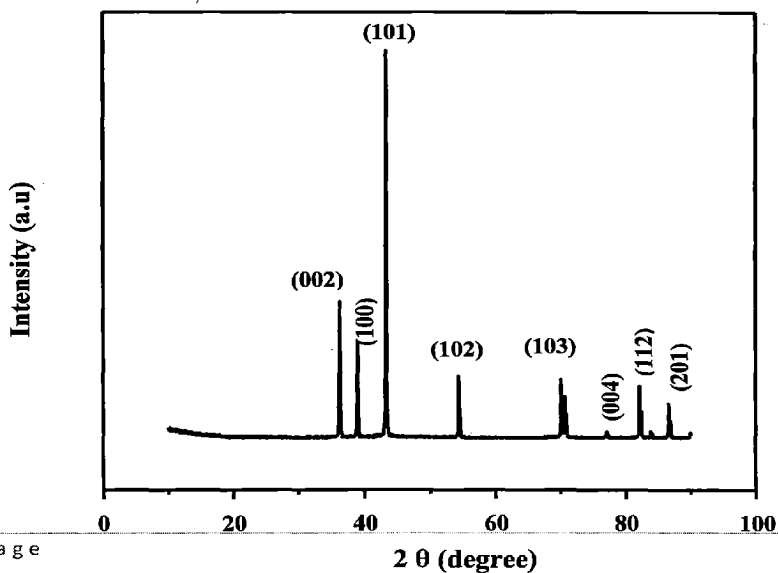


Fig: 4.2 Zn Powder XRD



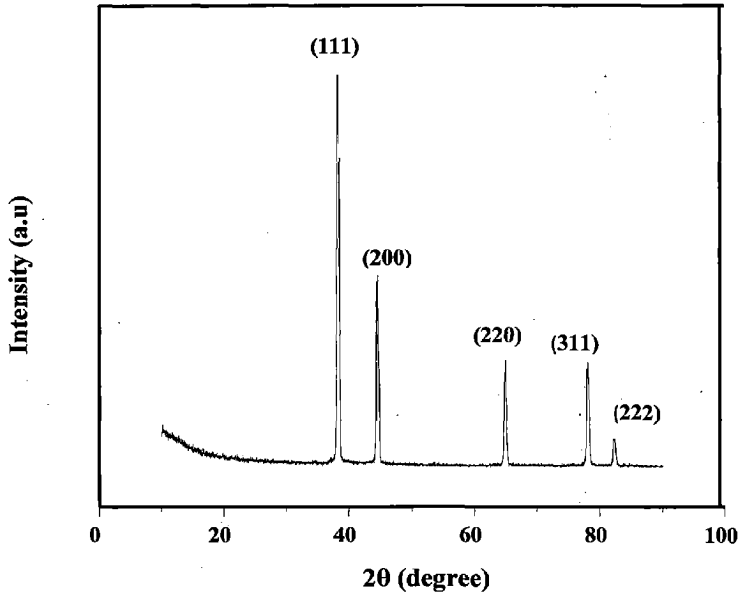


Fig: 4.3 Al powder XRD

Time(hr)	2hr	8hr	16hr	24hr	28hr	34hr	40hr	48hr
Cu Zn Al Lattice Parameter(Å)	3.6258	3.6196	3.6120	3.6158	3.6305	3.6248	3.6376	3.6225

Table: 4.2 Variation of Lattice Parameter of Cu with variation of milling time in hour

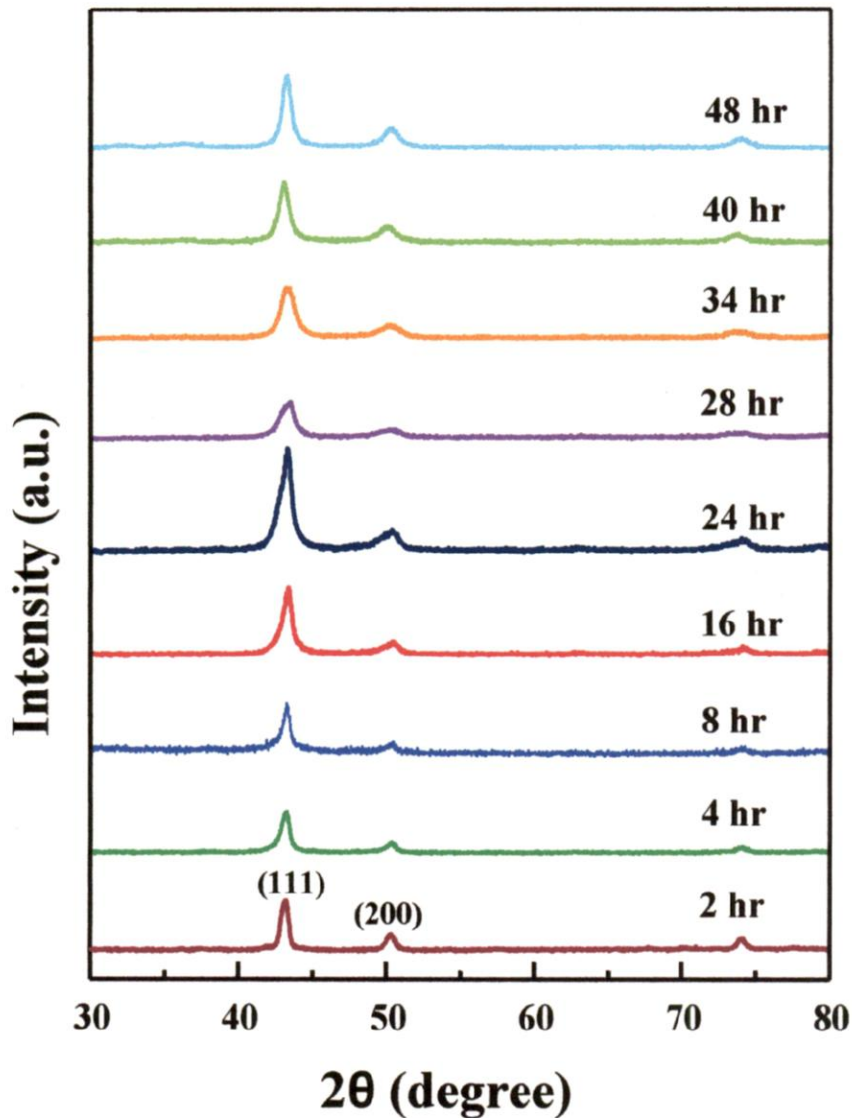


Figure: 4.4 XRD patterns of the prepared samples.

4.1 X-Ray Diffraction Analysis

Figure 4.1 shows the XRD pattern of the prepared samples. The pattern shows dominant (111) diffraction peak along with low intensity (200) diffraction peak. A reduction in particle size with increase of milling hours has been observed. Rate of particle size reduction is maximum for first 2 hr of milling. After that moderate size reduction observed. Grain (particle) reduction calculated by using Scherrer formula by measuring widening of prominent peak. Another phenomenon which is observed is decrease of gradual relative intensity of

secondary peaks with the respect of milling hrs; it is obvious outcome because some part of zinc and aluminum dissolves in copper. Dissolution of zinc into copper is not complete due to structural constraints. Dissolution of zinc and aluminum is maximum up to 28 hrs of milling stage. With further milling grain size reduction reversed. At 24 hrs milling stage liquid nitrogen introduced in material to cool down material substantially and enhance particle reduction and optimize lattice strain. During 4 hrs of milling in liquid nitrogen medium there has been maximum particle size reduction and maximum lattice strain, in fact it is optimized condition observed. With further milling hrs in liquid nitrogen, there has been increase in particle size and thus decrease in lattice strain and thus increase in relative intensity of peaks. This reversed phenomenon observed due to evolution of heat while readjustment of grain boundaries, release of surface energy earlier stored along grain boundaries and mechanical work done by balls continuously striking material.

In particle size with increase of milling hours has been observed. Rate of particle size reduction is maximum for first 2 hr of milling. After that moderate size reduction observes. Grain (particle) reduction calculated by using Scherer formula by measuring widening of prominent peak. Another phenomenon which is observed is decrease of gradual relative intensity of secondary peaks with the respect of milling hrs; it is obvious outcome because some part of zinc and aluminum dissolves in copper. Dissolution of zinc into copper is not complete due to structural constraints. Dissolution of zinc and aluminum is maximum up to 28 hrs of milling stage. With further milling grain size reduction reversed. At 24 hrs milling stage liquid nitrogen introduced in material to cool down material substantially and enhance particle reduction and optimize lattice strain. During 4 hrs of milling in liquid nitrogen medium there has been maximum particle size reduction and maximum lattice strain, in fact it is optimize condition observed. With further milling hrs in liquid nitrogen, there has been increase in particle size and thus decrease in lattice strain and thus increase in relative

intensity of peaks. This reversed phenomenon observed due to evolution of heat while readjustment of grain boundaries, release of surface energy earlier stored along grain boundaries and mechanical work done by balls continuously striking material.

4.2 Graph Particle Size V/S Milling Hours

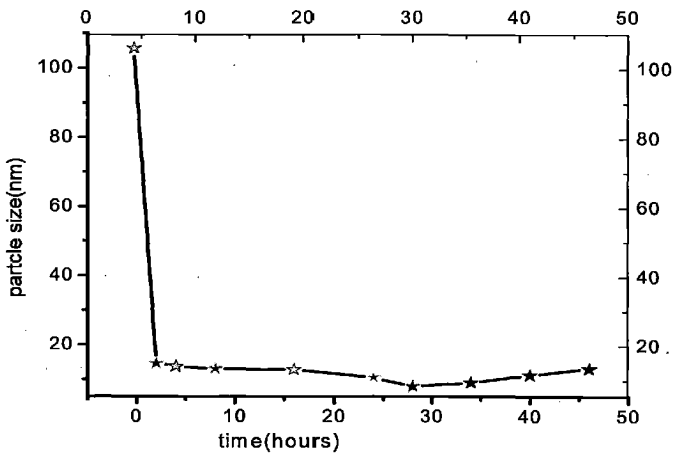
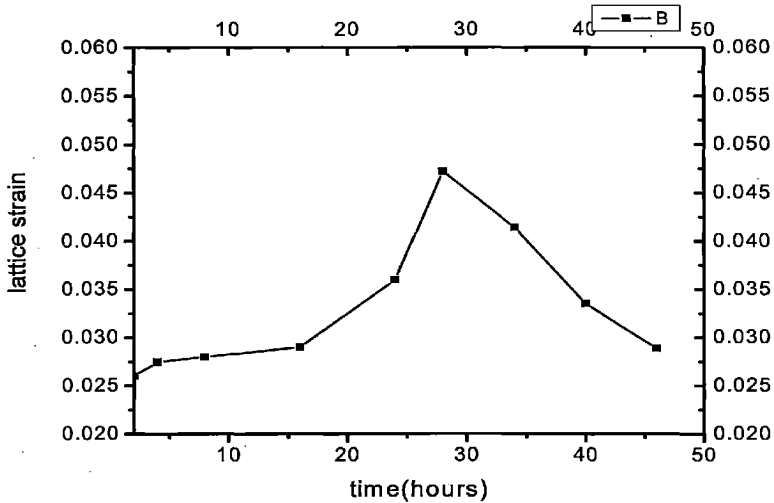


Fig: 4.2

In first two hours of milling particle size steeply decreases then it reduces gradually up to 24 hours of milling, from 24 hours to 28 hours there has been rapid decrease of particle size. In this time interval milling was done with liquid nitrogen medium. Liquid nitrogen decreases temperature of material and enhances brittleness thus decreasing particle size rapidly. After 28 hours of milling there has been gradual increase of particle size. This anomalous behavior can be explained on the basis of max. Cold working energy stored in the region of grain boundaries. At 28 hours of milling stage energy stored in the region of grain boundaries is max. Further milling enhances grain growth and readjustment of grain boundaries with release of energy stored, temperature increases.

4.3 Lattice strain v/s milling hours

Fig: 4.3



Lattice strain gradually increases with respect to milling time, as particle size decreases. Behavior of graph is reciprocal in nature corresponding to particle size v/s milling hour graph. Lattice strain is reciprocal to particle size, so same explanation is applicable as it is used for particle size v/s milling hours.

4.4 Scanning Electron Microscopy (SEM):

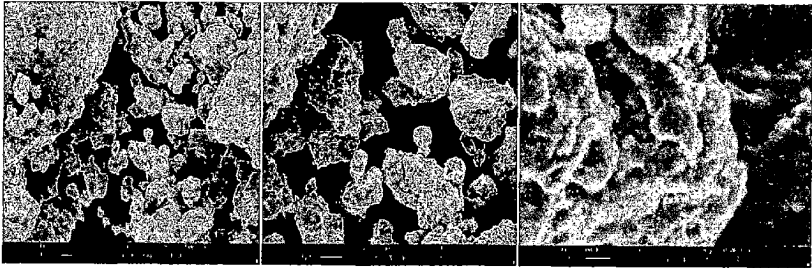


Fig (4.4a) 2hr milled sample viewed 500X, 1000X, 5000X magnification

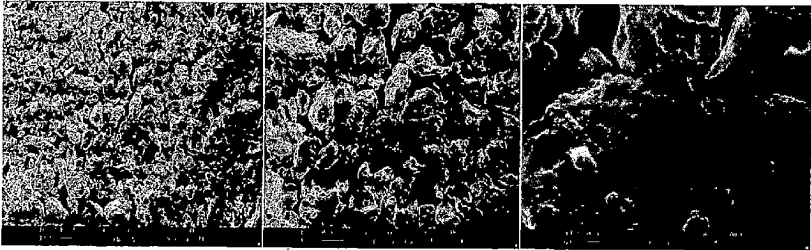


Fig (4.4b) 4 hr milled sample under 500X, 1000X, 5000X magnification

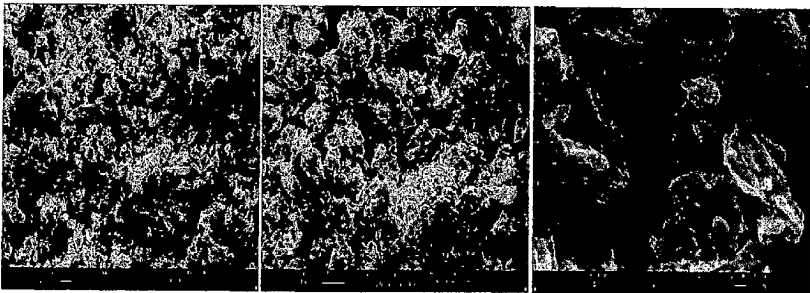


Fig (4.4c) 16 hr milled sample under 500X, 1K, 5K magnification

Morphology of material at two hr milling stage shows porous aggregation, in layered structure. Further milling cause severe plastic deformation to small aggregates to form

layered structure. Further severe plastic deformation causes elongated flaky- particle, fragmented to small particles. Results show that size reduction around 24 hours to 28 hours is max. Further size reduction not observed after 28 hour of milling.

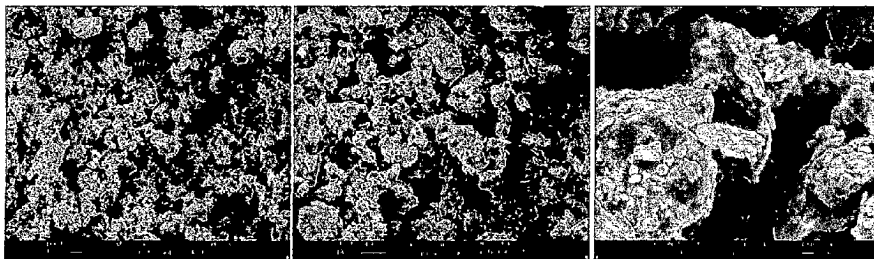


Fig (4.4d) 24 hours milled sample under 500X, 1K, 5K magnification

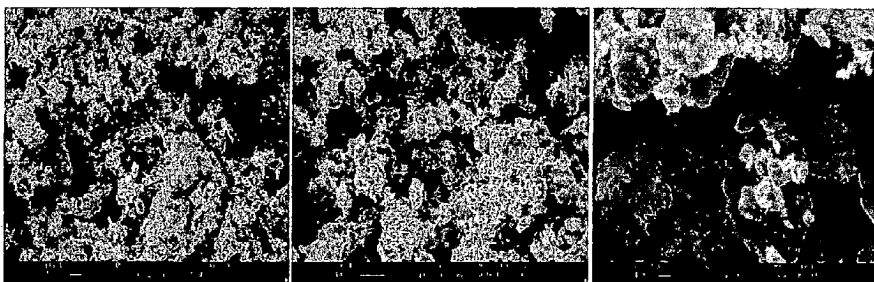


Fig (4.4e) 28 hours milled sample under 500X, 1k, 5k magnification

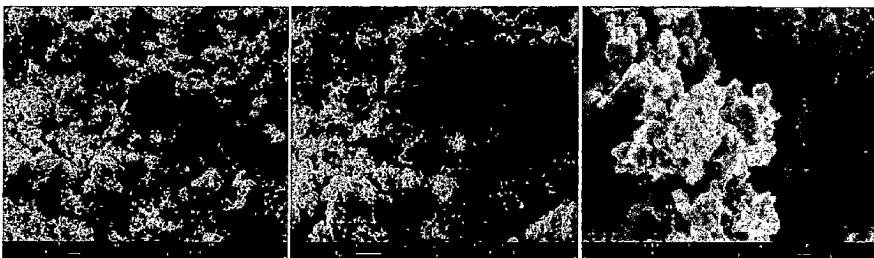


Fig (4.4f) 34 hours milled sample under 500X, 1K, 5K, magnification

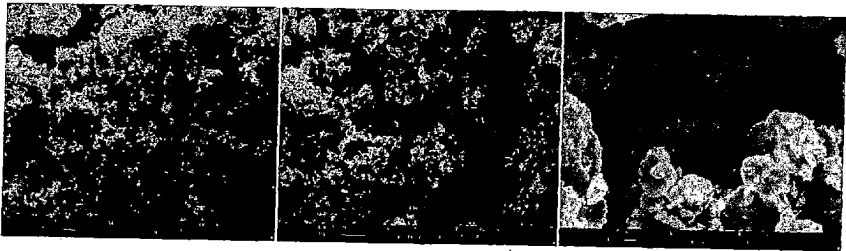


Fig (4.4g) 40 hours milled sample under 500X, 1K, 5K magnification

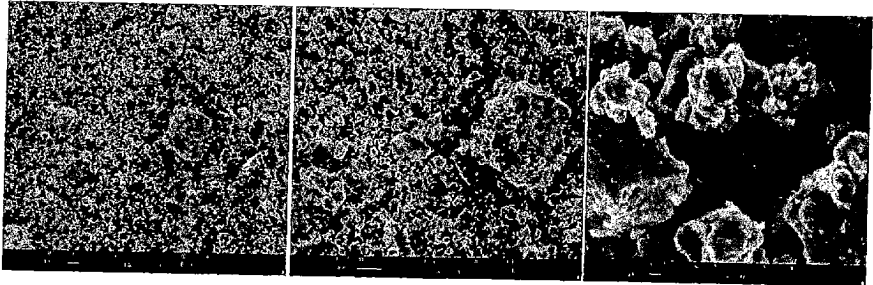


Fig (4.4h) 46 hours milled sample under 500X, 1K, 5K magnification

More heterogeneity observed beyond 34 hrs milling. Bigger particle embedded with small particles appears. Heat releases due to restructuring of grain boundaries increases the temperature, causing agglomeration, welding, increase in ductility and increase of grain (particle diameter) observed in prolonged milling.

4.5 FE-SEM (Field Emission Electron Microscopy)

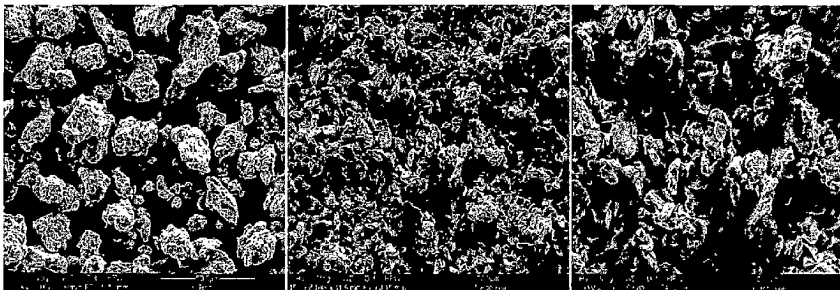
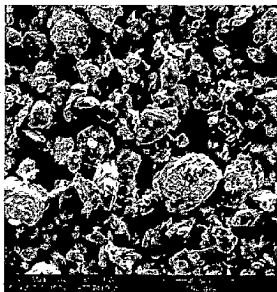


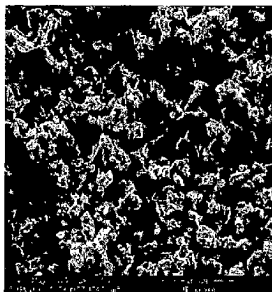
Fig (4.5a) 2hr (1000X)

16hr (1000X)

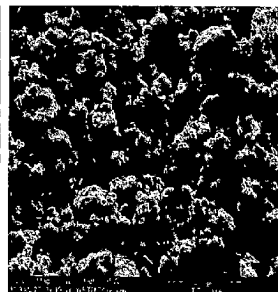
16hr (2000X)



24hr (2Kx)



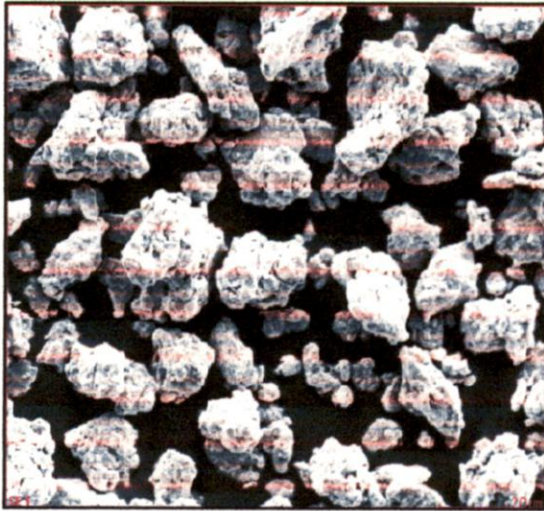
28hr (2Kx)



40hr (2kX)

FESEM images of the prepared samples

4.6 EDAX (Energy Dispersive X-Ray Analysis)



Element	Wt%	At%
AlK	4.53	10.12
CuK	68.73	65.23
ZnK	26.74	24.65
Matrix	Correction	ZAF

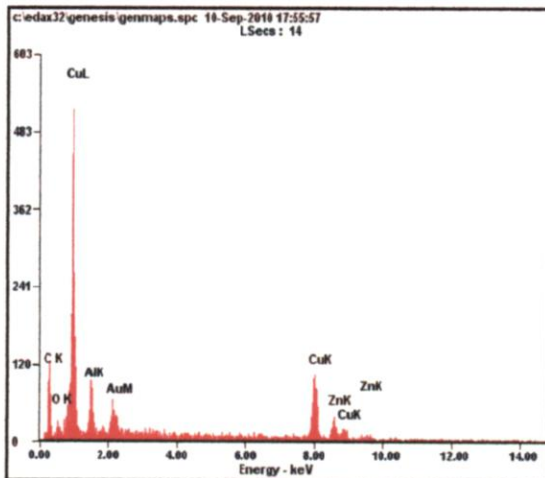
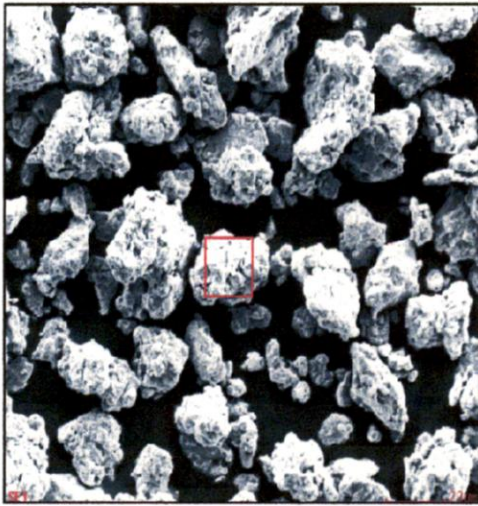


Figure: 4.6a EDAX pattern of 2hr milling



Element	Wt%	At%
AlK	3.09	7.03
CuK	73.75	71.23
ZnK	23.14	21.73
Matrix	Correction	ZAF

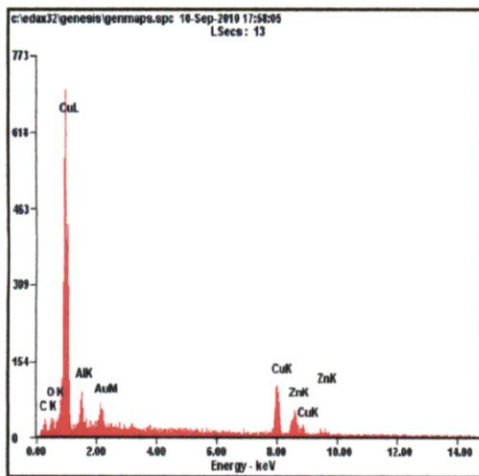
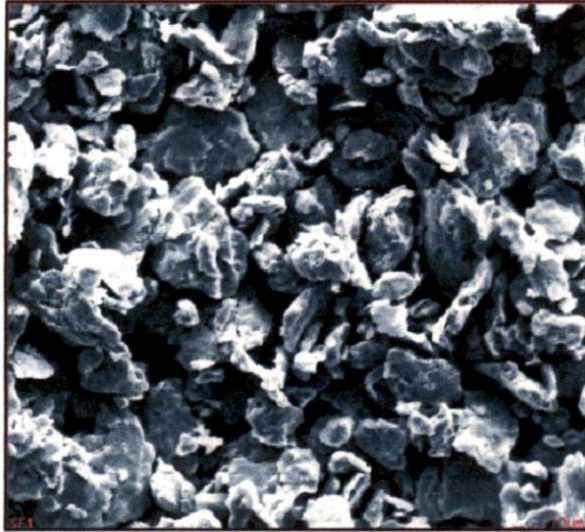


Figure: 4.6b EDAX pattern of 2hr milling of selected grain



Element	Wt%	At%
AlK	4.08	6.42
CuK	57.72	56.94
ZnK	38.2	36.63
Matrix	Correction	ZAF

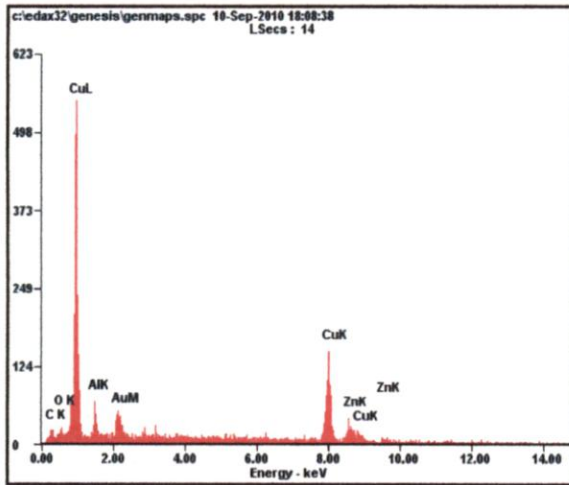
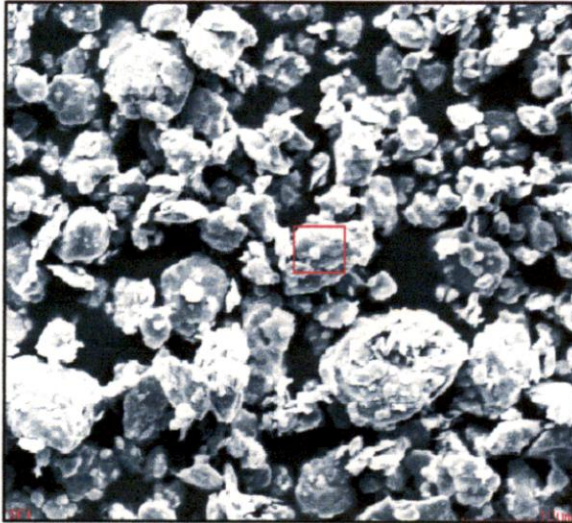


Figure: 4.6c EDAX pattern of 16 hr milling



Element	Wt%	At%
AlK	02.86	06.52
CuK	75.22	72.85
ZnK	21.90	20.62
Matrix	Correction	ZAF

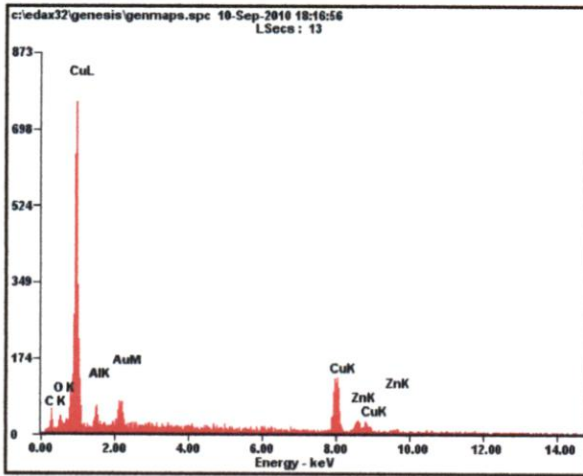


Figure: 4.6dEDAX pattern of 24hr milling of selected grain



Element	Wt%	At%
AlK	03.40	07.70
CuK	73.90	71.09
ZnK	22.69	21.22
Matrix	Correction	ZAF

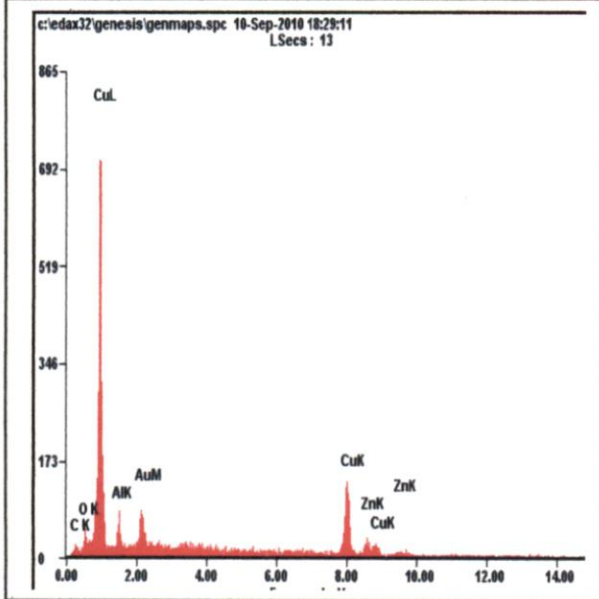
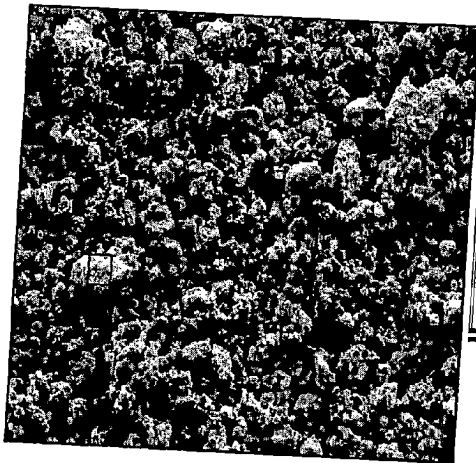


Figure: 4.6eEDAX pattern of 28 milling of selected grain



Element	Wt%	At%
AlK	03.24	06.66
CuK	69.96	68.24
ZnK	26.49	25.11
Matrix	Correction	ZAF

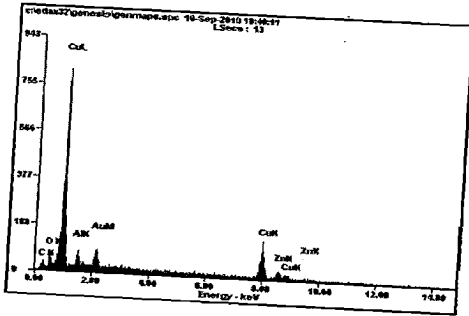


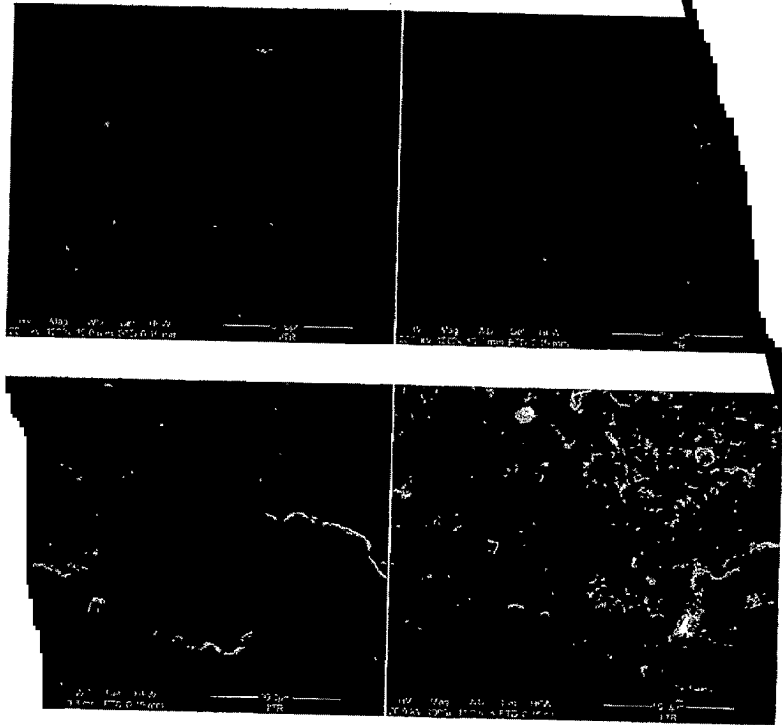
Figure: 4.6f EDAX pattern of 40hr milling of selected grain

EDAX-ANALYSIS

Energy dispersive X-ray analysis is an analytical technique used for elemental analysis or chemical characterization of a sample. It is one of the variants of X-ray fluorescence spectroscopy which relies on the investigation of a sample through interactions between electromagnetic radiation and matter, analyzing X-ray emitted by the matter in response to being hit with charged particles.

The most significant issue to note from this is that X-ray generated from any particular element are characteristic of that element, and as such, can be used to identify which elements are actually present under the electron probe. This is achieved by constructing an index of X-rays collected from a particular spot on the specimen surface, which is known as spectrum. Software is capable to analyze number of elements present in the sample with their individual percentage. Thus EDX analysis is very useful in determining the contamination present in sample and also very useful to analyze level of mixing in alloy formation, if alloy is homogeneous then elemental proportion must remain constant at each point of the material. In our work we have taken Cu-Zn-Al sample in the ratio of wt% 72,22,4 respectively as milling time increases particle compositions in terms of weight reaches to equilibrium, since spots are randomly selected for EDAX. Results also emphasize that with increase of milling time solid solution also becomes homogeneous. Results are in accordance with expectation.

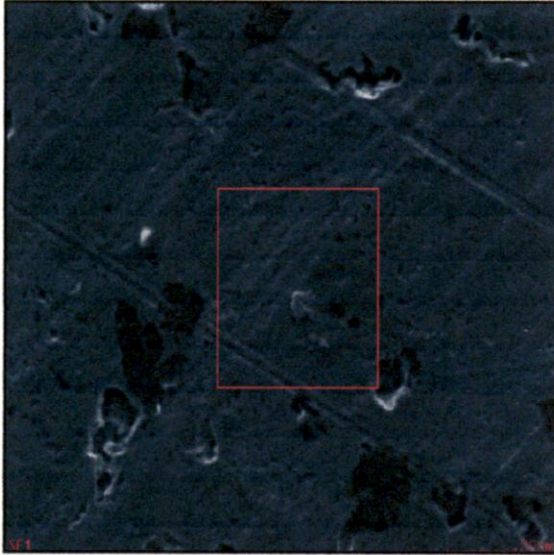
FE-SEM AND EDAX OF SINTERED Temperature 500°C for 1 hr in H₂ environment



Micrographs of sintered Pellets (from top to bottom), as mixed, 2hr, 20hr, 48hr

SEM pictures shows that in as mixed samples, there is no grain formation, it is only two hr milled sample, some grain formation of heterogeneous nature has glomeration of small particles into larger one. Particle size of 1 μ and bigger is observed. In 20 hr milled sample, grains are bigger in size, more homogeneous. In 48 hr milled sample, particles are more heterogeneous in nature; there is highest variation in particle size as it appeared in 48 hr milled powder sample. Prolonged milling created dislocation and release of heat stored along grain boundaries is cause behind agglomeration.

EDAX PATTERN:



Element	Wt%	At%
AlK	04.82	10.67
CuK	70.84	66.78
ZnK	24.34	22.56
Matrix	Correction	ZAF

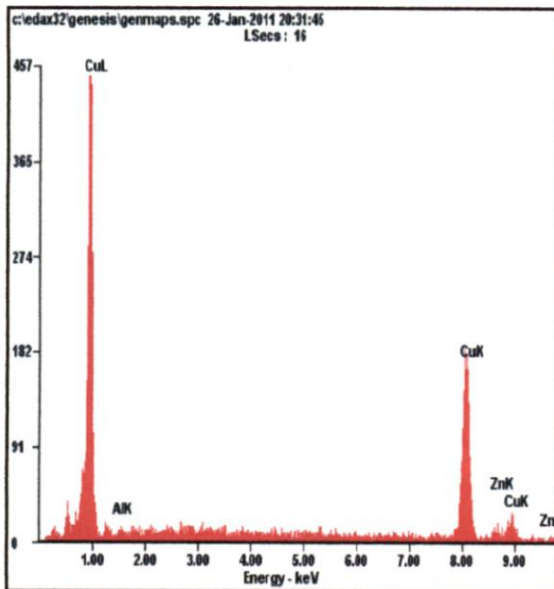
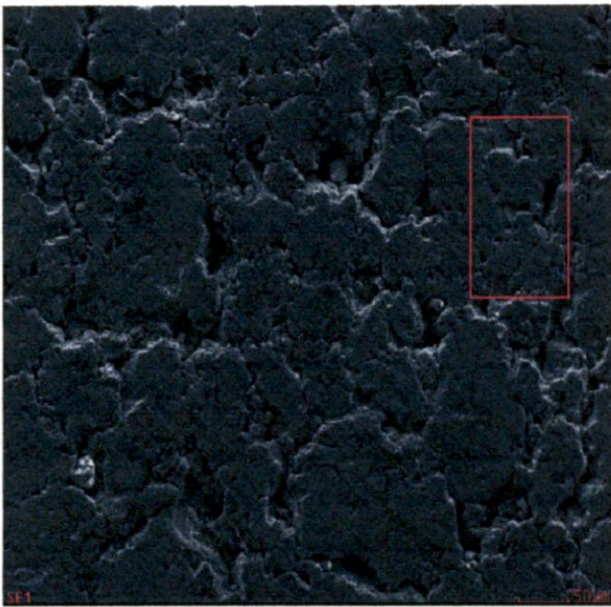


Fig: 4.7b EDAX of as mixed powder pellet sintered for 1 hr in presence of H₂ environment

Analysis: EDAX analysis of as mixed sample shows composition of alloy. Cu phase is dominant one due to its prominent share. Zn and Al peaks are intense compare to strong peaks of Cu. It shows no solid solution of lesser constituents in Cu phase.



Element	Wt%	At%
AlK	05.52	12.18
CuK	69.10	64.72
ZnK	25.37	23.10
Matrix	Correction	ZAF

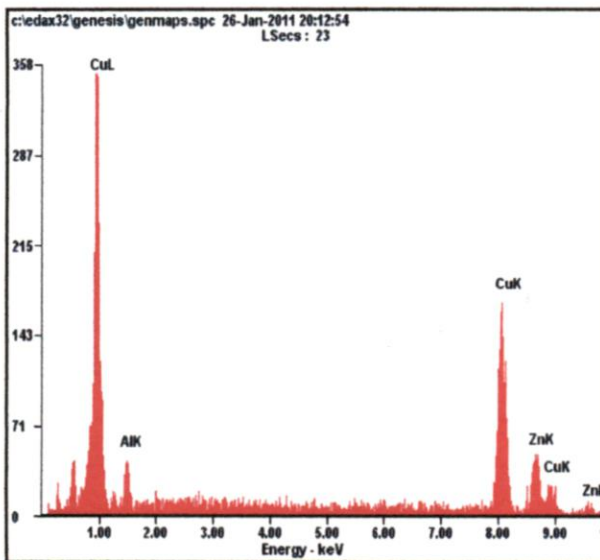
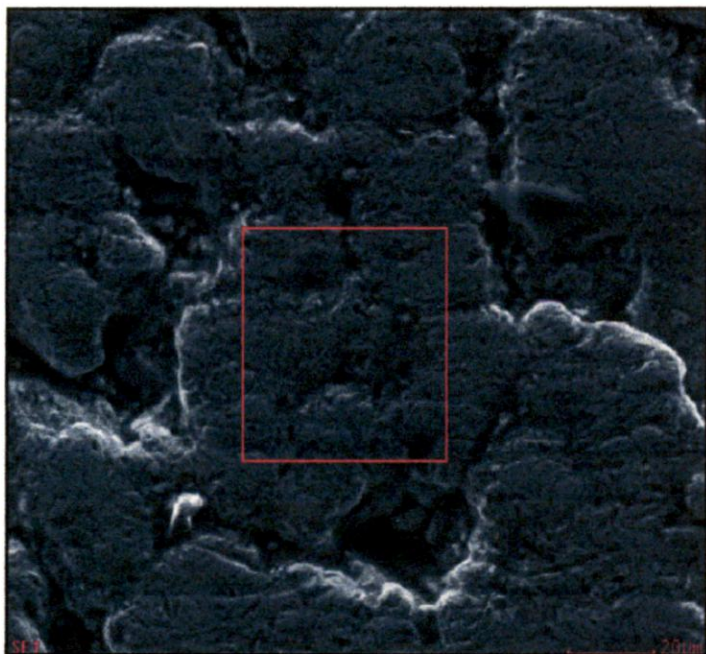


Fig: 4.7c EDAX of 2hr milled powder pellet sintered for 1 hr in presence of H₂ environment

Analysis: EDAX Analysis of selected area of region of two hr milled sample indicates

Increase of intensity of Zn and Al with respect to Cu peak. Relative intensity of Cu peaks decreases with respect to lesser constituents. This is in accordance with increase of weight percent of Zn and Al with respect of Cu. This phenomenon is due to solid solution of Zn and Al in copper.



Element	Wt%	At%
AlK	07.22	15.58
CuK	69.13	63.35
ZnK	23.65	21.06
Matrix	Correction	ZAF

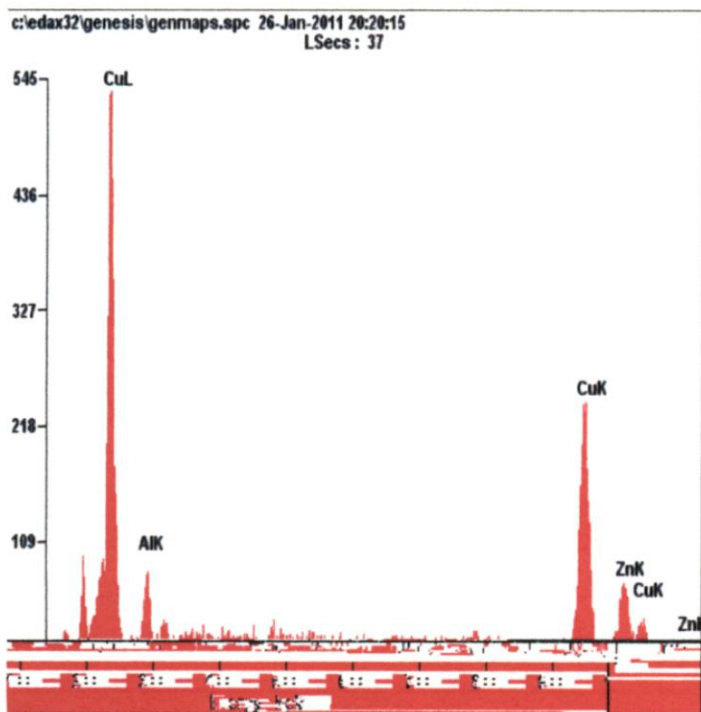
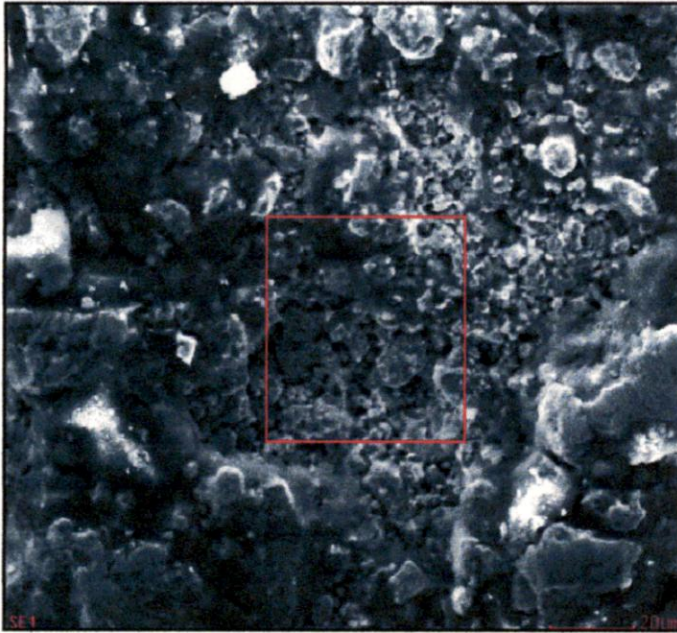


Fig: 4.7d EDAX of 20hr milled powder pellet sintered for 1 hr in presence of H₂ environment

Analysis: EDAX pattern of 20 hr milled pattern of sintered sample is almost same as earlier 2 hr milled sample. There is relative increase of intensity of Al constituent with respect to Cu and Zn constituent. Due to hexagonal structure and lattice parameter of Zn it is less soluble in copper than face centered Al, more soluble in Copper. Al atom substituted Zn atoms as milling time increases and subsequently sintering process.



Element	Wt%	At%
AlK	06.06	13.27
CuK	70.51	65.56
ZnK	23.43	21.17
Matrix	Correction	ZAF

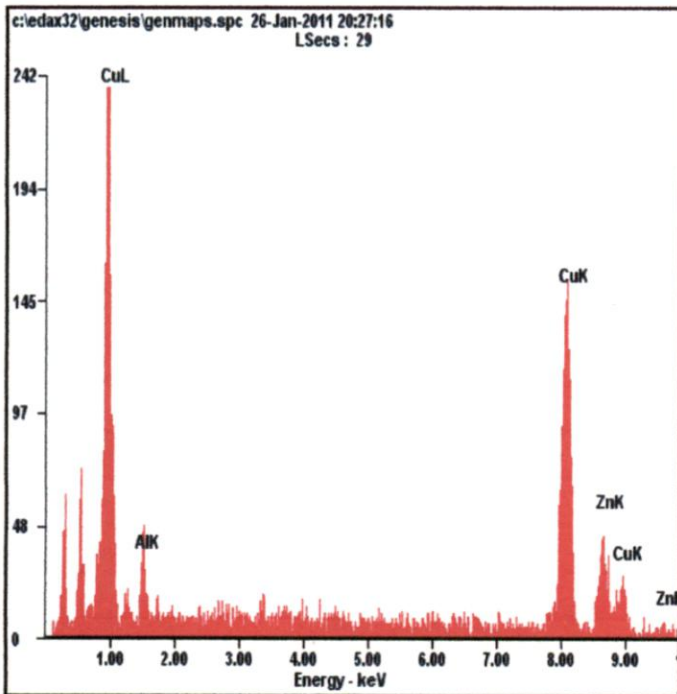


Fig: 4.7e EDAX of 48hr milled powder pellet sintered for 1 hr in presence of H₂ environment

Analysis: EDAX OF 48 hr milled sintered sample, there is reverse formation, and there is again relative increase of Cu with respect Zn and Al, due to excess formation of heat, agglomeration takes place, structure is heterogeneous in nature. Solubility of Al and Cu is almost invariant with respect to milling time after reaching a saturation stage.

4.8 Density V/S Milling hrs Graph for Sintered Pellets:

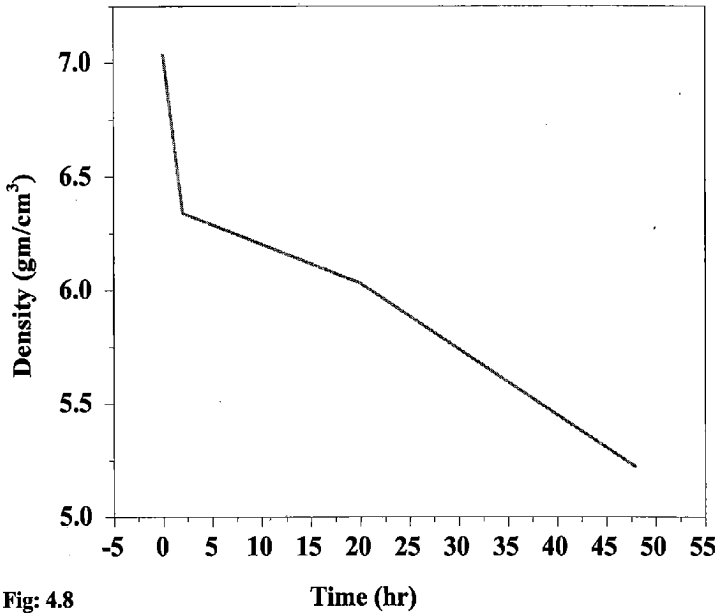


Fig: 4.8

Analysis: density of sintered pellets decreases with milling hr. this phenomenon can be explained on the basis of increase of surface area per unit volume with decrease in particle size. Since pressure applied is same for making all pellets density is lowest for that sample which was milled for maximum time, its particle size is lowest.

4.9 Microhardness v/s milling hrs Graph:

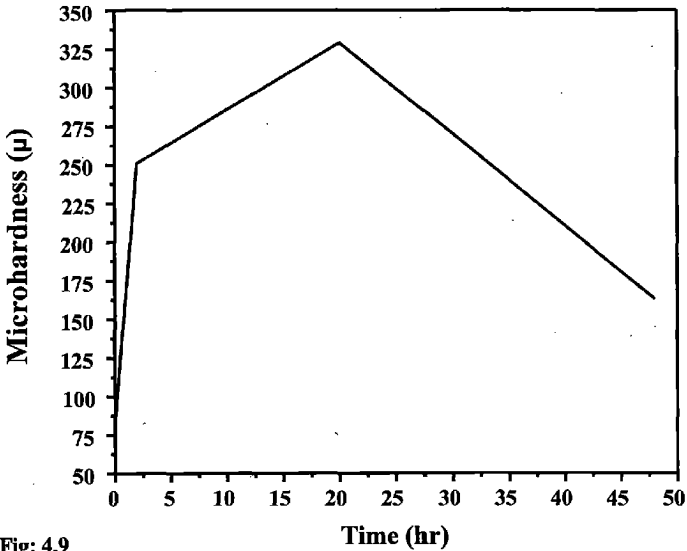


Fig: 4.9

Analysis:

Variation of micro hardness with milling time in hrs can be explained on the basis of Hall-Petch & reverse Hall-Petch effect.

$$\sigma_0 = \sigma_I + k D^{-1/2}$$

Where σ_0 = the yield stress

σ_I = the “friction stress,” representing the overall resistance of the crystal lattice to dislocation movement.

K = the “locking parameter,” which measures the relative hardening contribution of the grain boundaries

D = grain diameter

This equation also applicable to measure hardness of the material with adjustment of suitable constant. As particle diameter decreases, hardness increases and max for Hall-Petch limit, that is about 12nm. The weakening of the material, due to the shift in the dominant

mechanism of plastic deformation in the coarse- grained materials to GB sliding in the case of ultra-small grain sizes, is referred to as the inverse Hall-Petch behavior.

4.10 Hot Forging and Rolling:

We performed hot forging and rolling operation in order to develop stabilized martensitic phase in material in order to develop shape memory effect. After hot rolling we simply found that material is too brittle to deform it in thin sheet, so physical verification of shape memory effect is not possible by powder metallurgy route and HEBM. Nanostructure cannot be retained in hot forging and hot rolling.

4.11 Optical Metallography: An Analysis

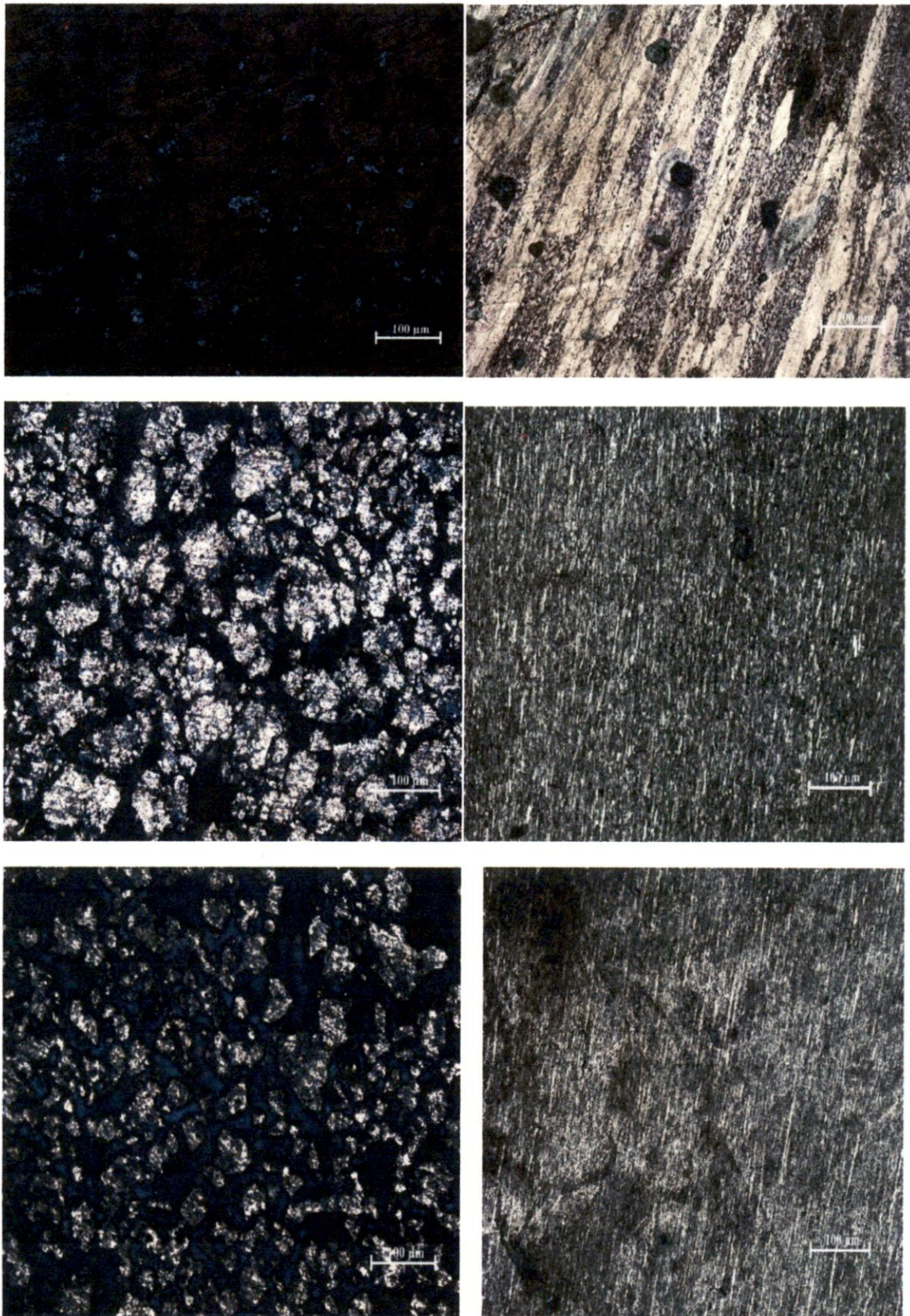
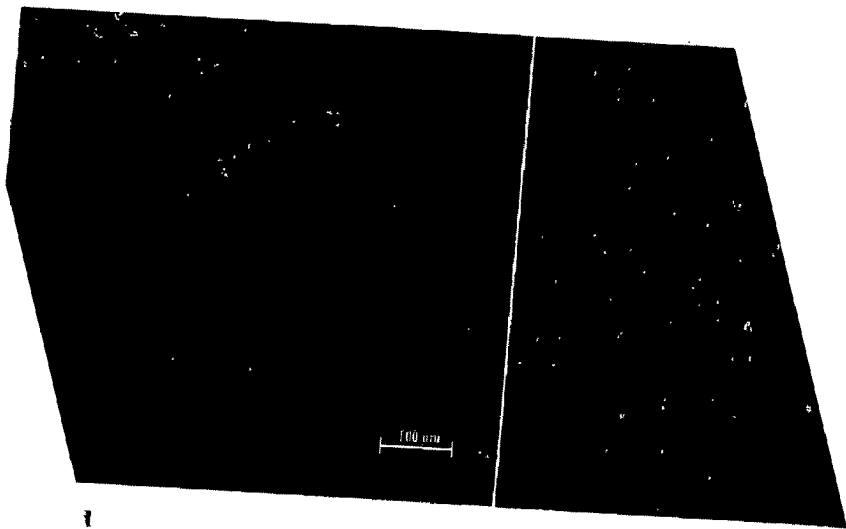


Fig: 4.11 a, b and c

... from two in groups: (1.) as mixed sintered,
... and forged. (3.) 20 hr sintered and forged



ed and forged sample

Optical Metallographs above shows difference in morphology of grain structure of grains for milled sintered sample and hot forged sample. In as milled sample shows that material is in two phase, grains are elongated along the direction of applied force in forging process. In 2hr and 20 hr sintered sample grains are finer, agglomeration of small particles into larger grains. In forged sample, it is difficult to trace two phase system, grain boundaries are not clear. Some stabilization of martensitic phase also takes place during cooling process. In 48 hr milled hot forged sample, grain boundaries are not clear, morphology is heterogeneous but martensitic β is stabilized. A test.

4.11a. DTA/TGA Analysis

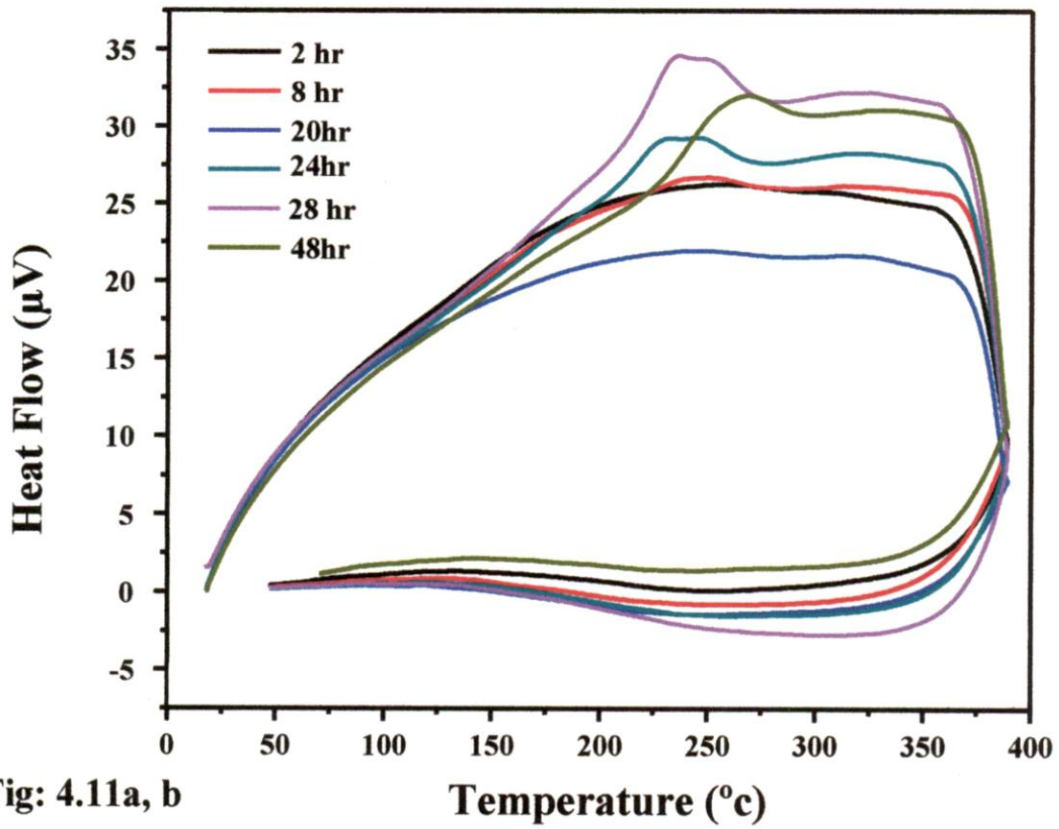
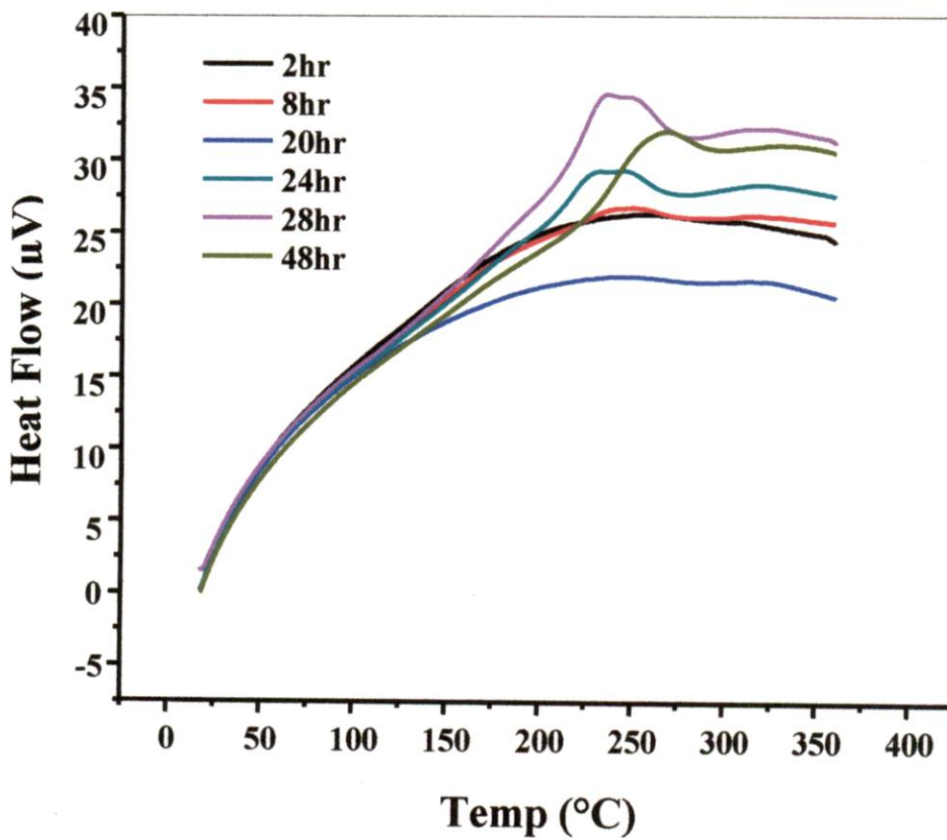
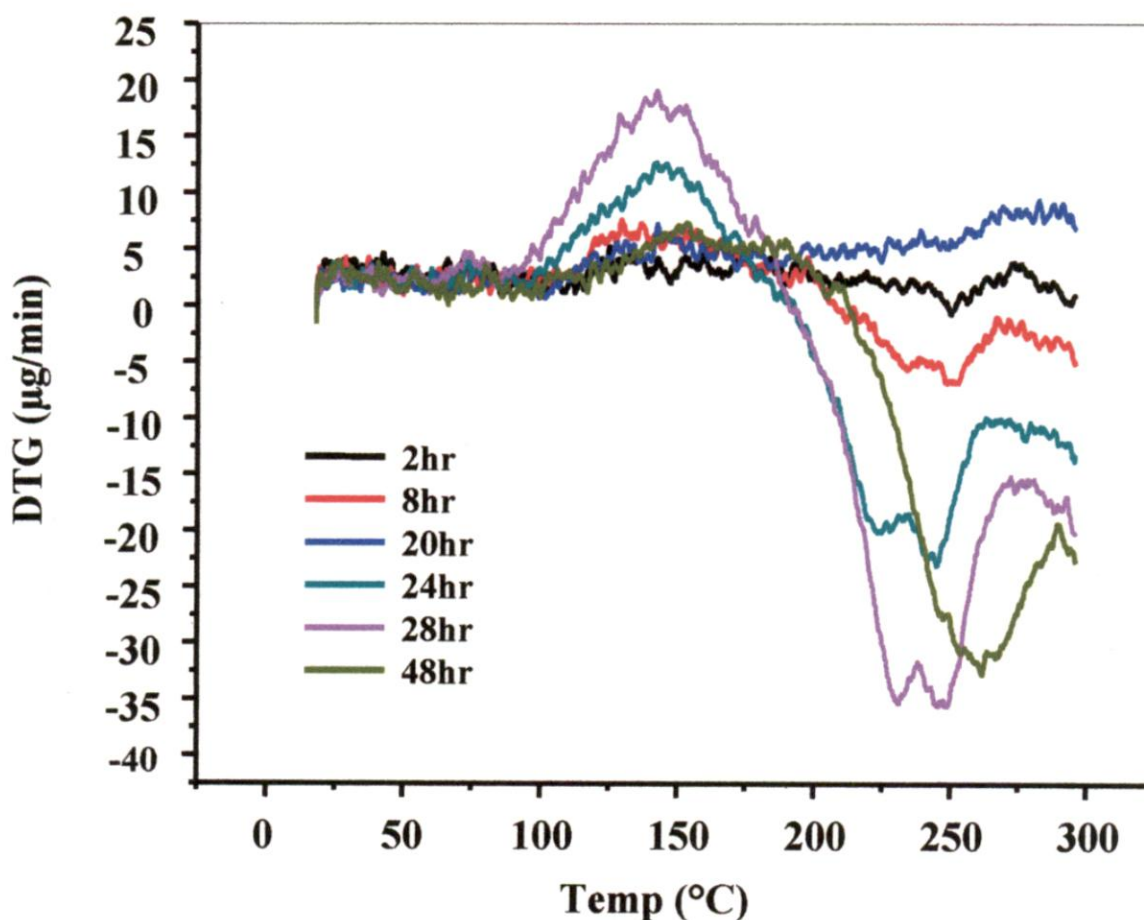


Fig: 4.11a, b



Analysis of heat flow curves for different samples having varying milling time shows that there is distinctive phase transformation temperature for 24, 28, and 48 hr milled samples. Particle size observed for 28 hr milled sample is minimum and quantity of heat flow is maximum for this sample also. There is maximum shift in peak temperature for this sample (236°C). T3-T1 (difference of temperature of peak initiation and end of peak) is minimum for 28 hr sample. This phenomenon is in accordance with nano crystallization effect. Heat flow peak is sharpest; temperature range of peak is minimum and overall decrease of peak occurring temperature. Transformation occurs in this range of temperature and peak is exothermic, heat is evolved due to phase transformation, some recrystallization process also occurs in transformation process.

4.11b. TGA Plots for various samples, heating only



TGA (Thermogravimetric Analysis) is a thermal analysis technique, which measures the weight change in a material as a function of temperature and time, in a controlled environment. In above graphs variation of weight change is maximum for 28 hr milled sintered sample. For 48hr sample, temperature at which maximum weight loss occurs is highest (263°C), all transition temperature for this sample are higher. DTA and DTG analysis

shows that phase transformation leads change of weight (gain or loss) for each sample. Weight gain or loss preceded phase transformation for each sample. Heat flow rate per unit mass is maximum for 28 hr sample, range of temperature for which transformation takes place is minimum for this sample. For 28 hr milled sample particle size is minimum and grain distribution is homogeneous in size. This sample may be better choice for application as shape memory alloy to fabricate devices for actuation purposes, provided grain size and distribution remains almost same in fabrication and further processing.

Table: Transition Temperatures for DTG Curves

Time(hr) milled Temp(°C)	24hr	28hr	48hr
T1	93	92	106
T2	143	142	145
T3	174	185	198
T4	225	232	263
T5	235	240	289
T6	245	248	310

Specifications of transformation temperatures:

T1 (initiation of weight gain), T2 (peak of weight gain), T3 (end of weight gain), T4 (peak of weight loss), T5 (reverse of peak weight gain), T6 (end of weight loss).

Range of temperature for which weight gain or loss is appreciably less for 28 hr sample and peaks are sharp and distinct compare to other sample and range has enough width to use for shape memory applications.

4.11c. TGA-Time Analysis

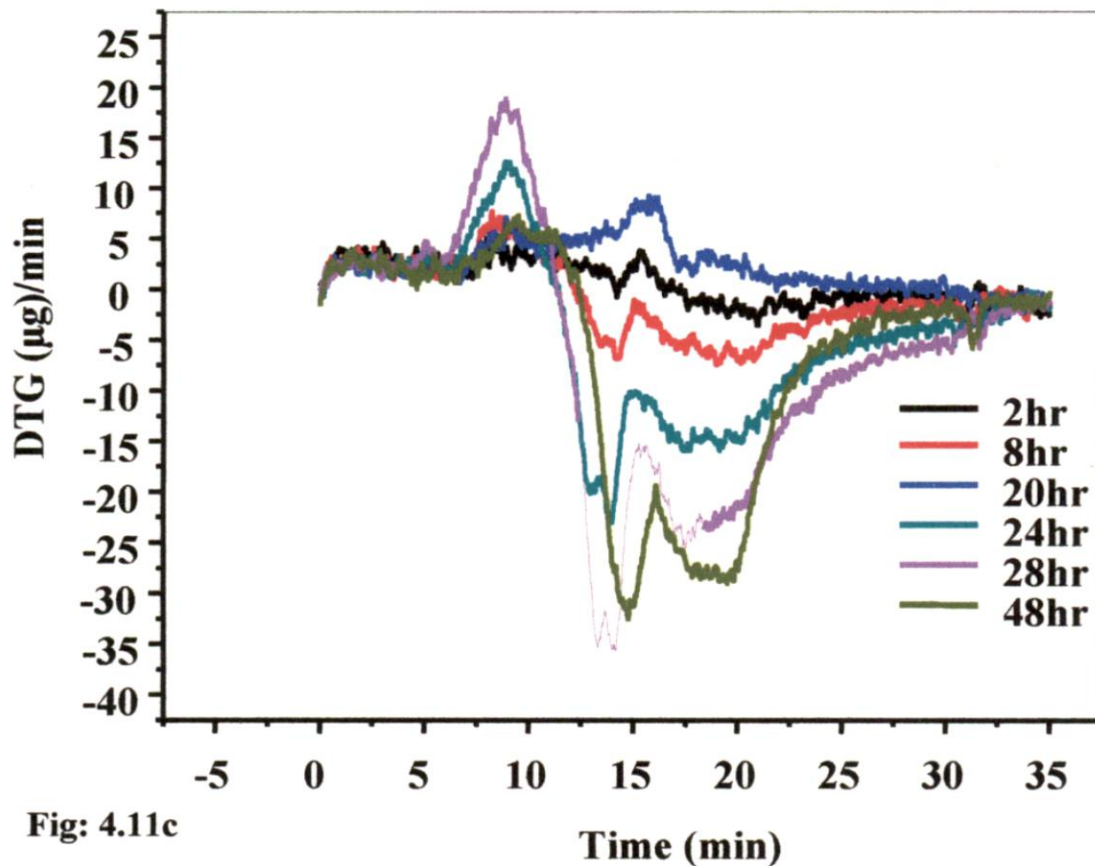


Fig: 4.11c

Since heating rate is constant and progressively constant, time and temperature runs parallel, time for maximum weight gain is almost same for 24,28 and 48 hr milled sample, it is higher for 20 hr milled sample. Time for maximum weight loss is same around 13 minutes for 24 and 28 hr milled sample. It is higher for 48 hr milled sample. Heterogeneity in structure, impurity, agglomeration of particles are causes behind observed shift in temperature and time for 48 hr milled sample.

4.11d. Milling hrs v/s Phase Transformations temperatures

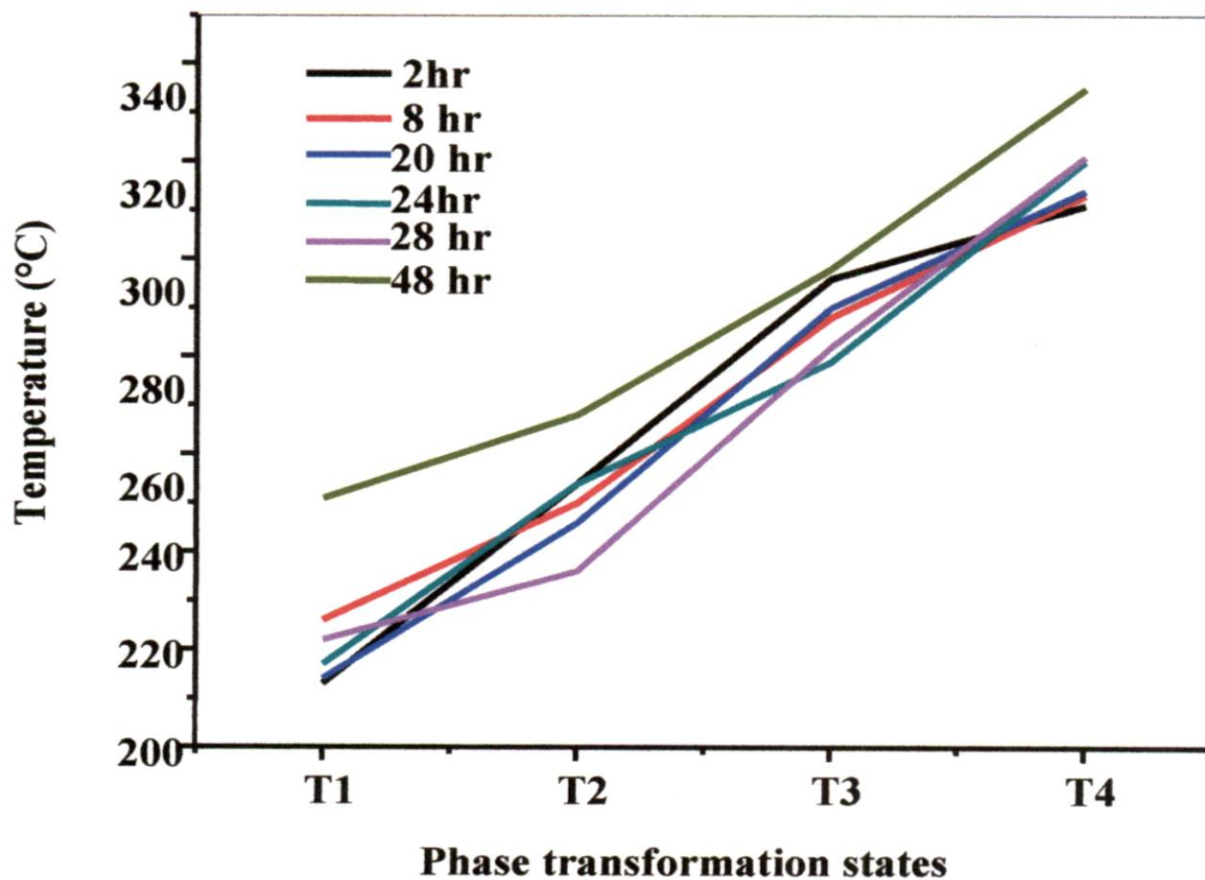


Fig: 4.11d

Table: 4.1

	2hr	8hr	20hr	24hr	28hr	48hr
T1	213	226	214	217	222	251
T2	254	250	246	254	236	268
T3	296	288	290	279	282	298
T4	311	313	314	320	321	335

Time(hr) Temp. (°C)	2hr	8hr	20hr	24hr	28hr	48hr
T2-T1	41	24	32	37	14	17
T3-T1	83	62	76	62	60	47
T4-T2	57	63	68	66	85	67

Table: 4.2

Among all samples of exothermic peak is maximum for 28 hr milled sample, while width is minimum except 48hr milled sample. Overall range of transformation temperature is maximum for 28 hr milled sample. Three samples give distinct transformation temperature for which sharp exothermic peaks can be observed with varying temperature ranges. We can select parameters according to temperature range required and magnitude of shape memory effect desired, but care is needed to fabricate the devices so that features of material remains invariant with processing.

4.11e.DTA Multiple Plot heating and cooling

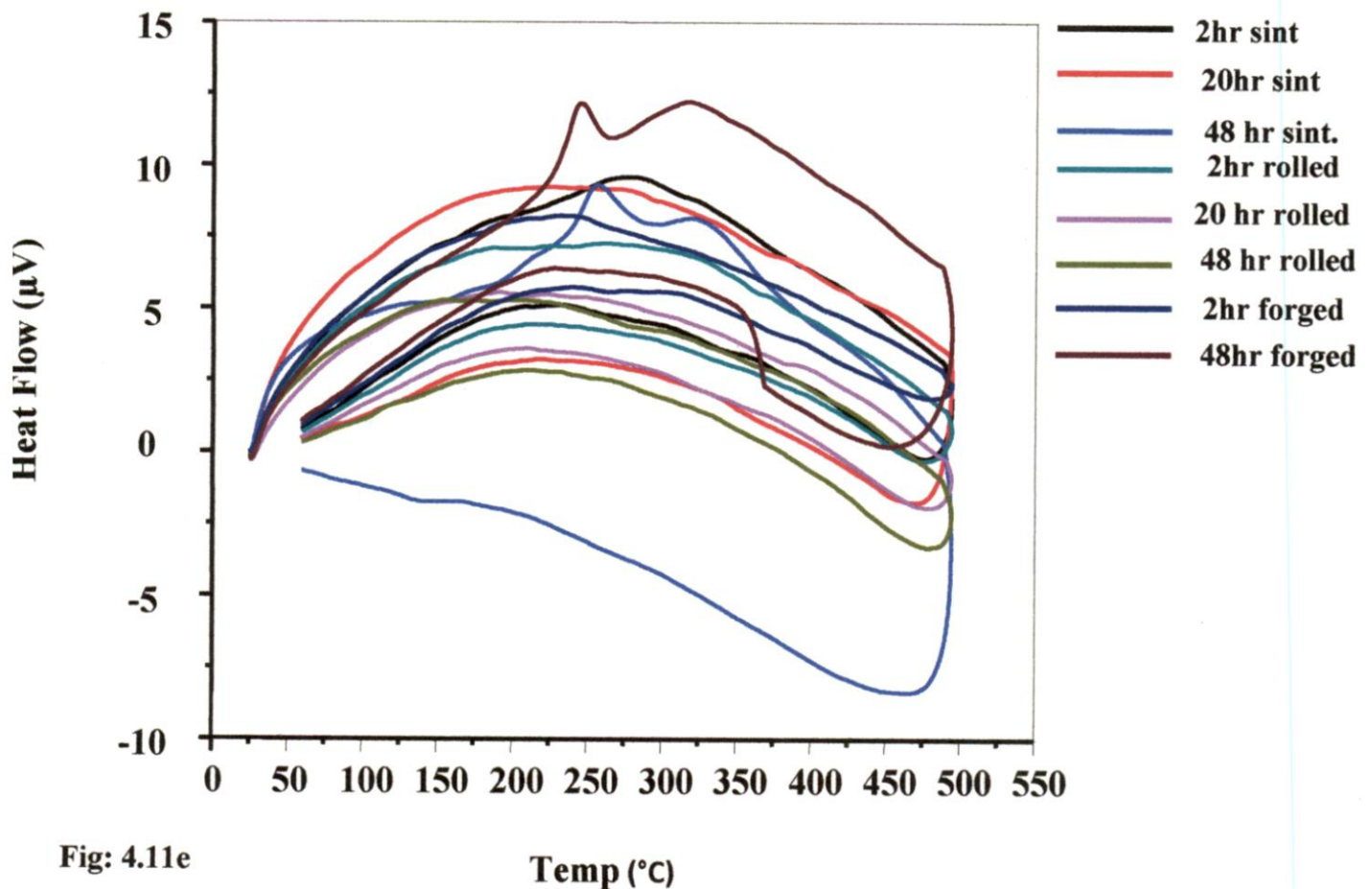


Fig: 4.11e

Now there is comparative analysis for samples having undergone different Thermomechanical treatment, sintering, hot rolling and hot forging. Among all 48 hr hot forged sample, exothermic peaks are sharpest one. Major peak also shifted towards left. For hot rolled sample there is no marked significant phase transformation phenomenon. Sintered and hot forged sample shows significant sharp exothermic peaks. Sintered sample cannot be directly used for fabrication of devices. Hot forged sample with suitable annealing, rolling and machining can be used to fabricate devices having appreciable SME. Sample 28 hr, 48 hr hot forged are best choice for SME having varying range of transformation temperatures

4.11f.DTA Multiple Plot heating

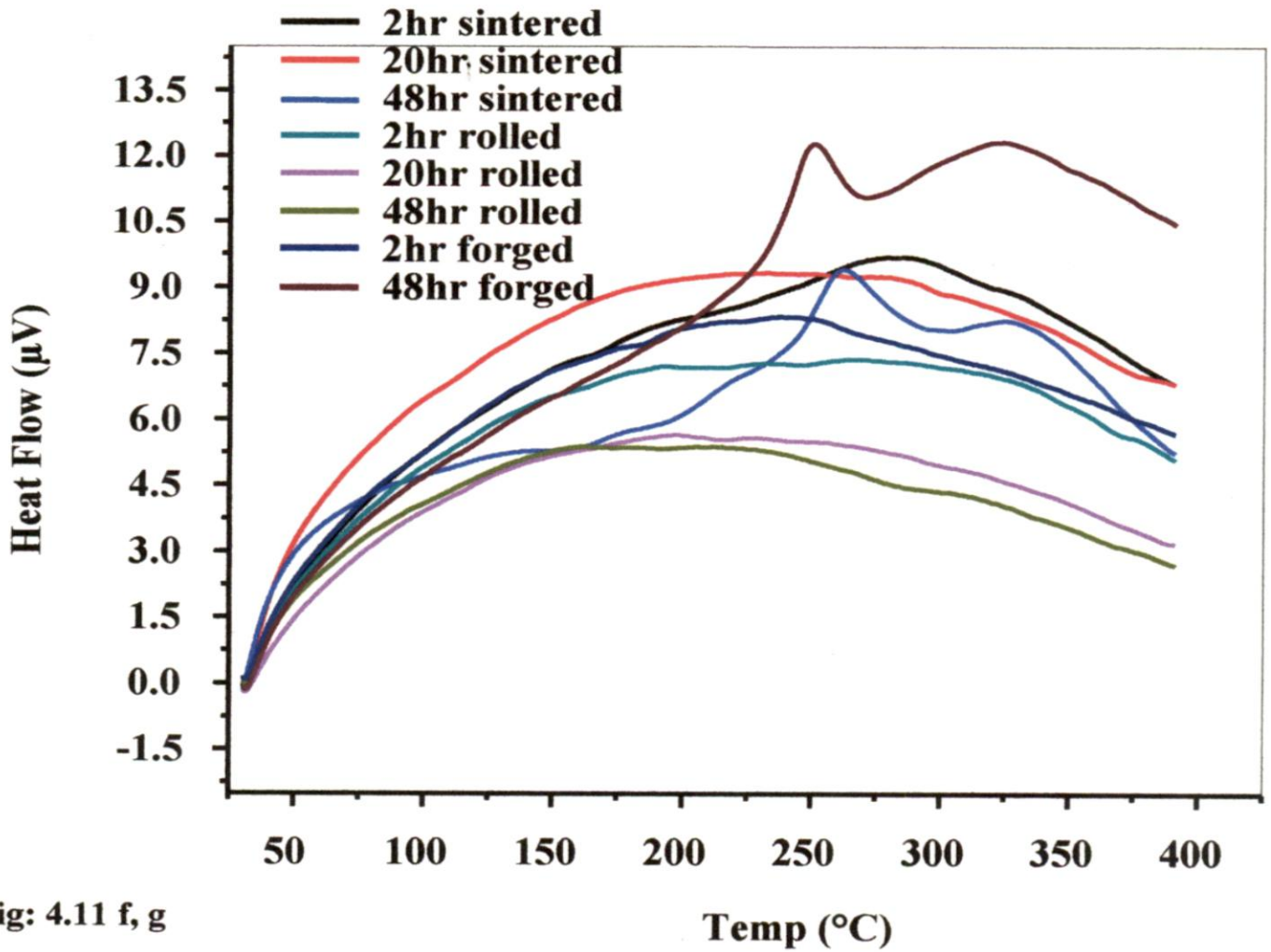
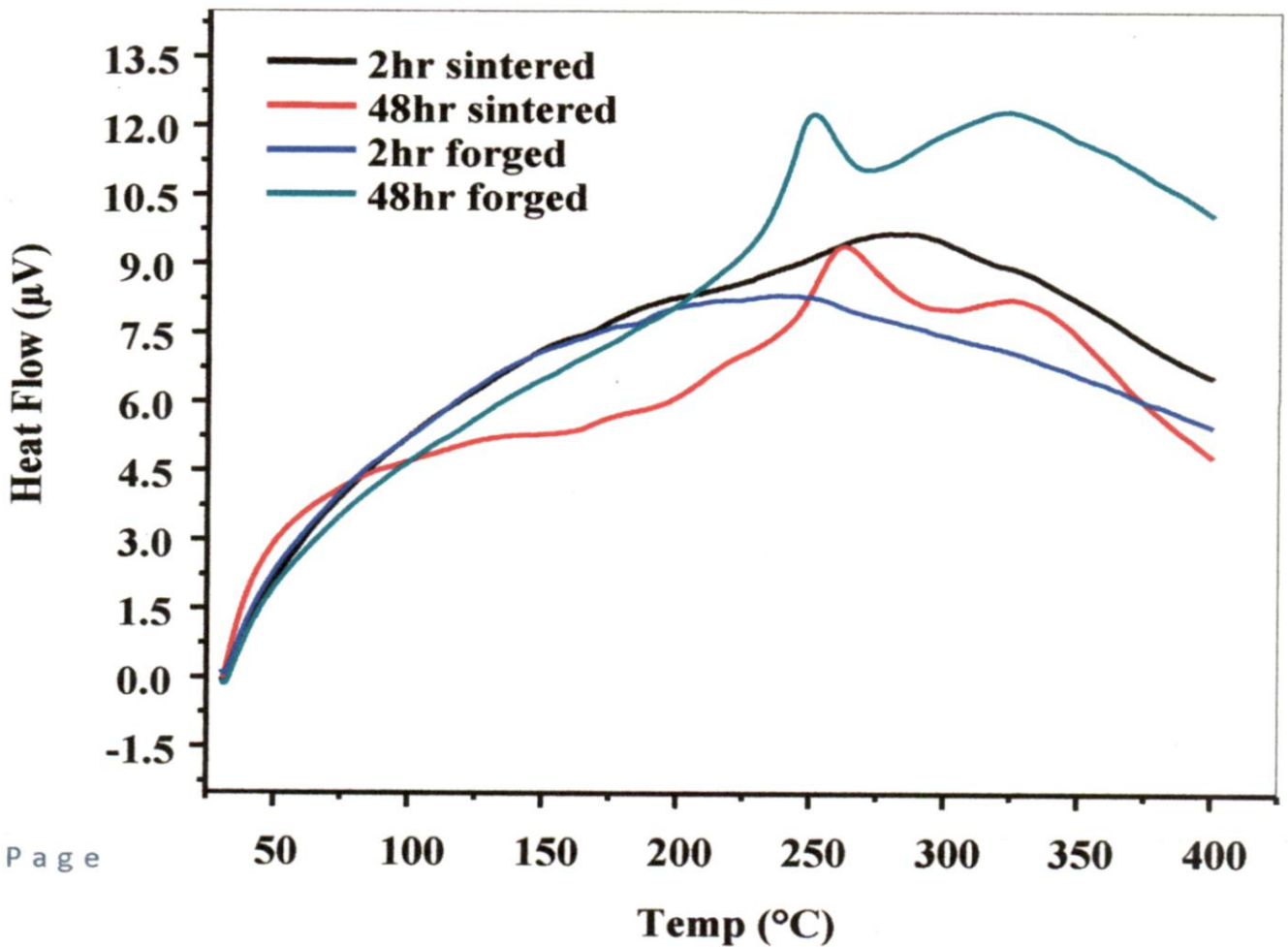
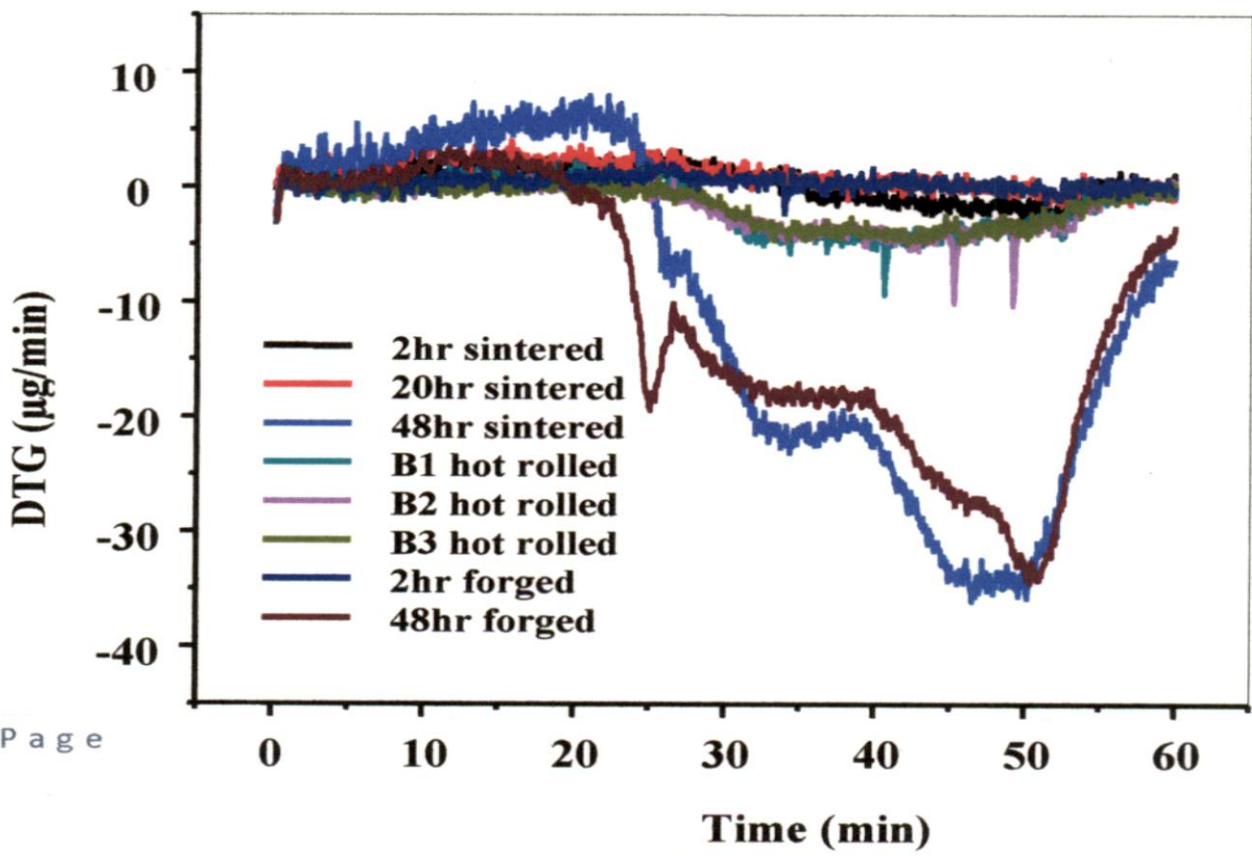
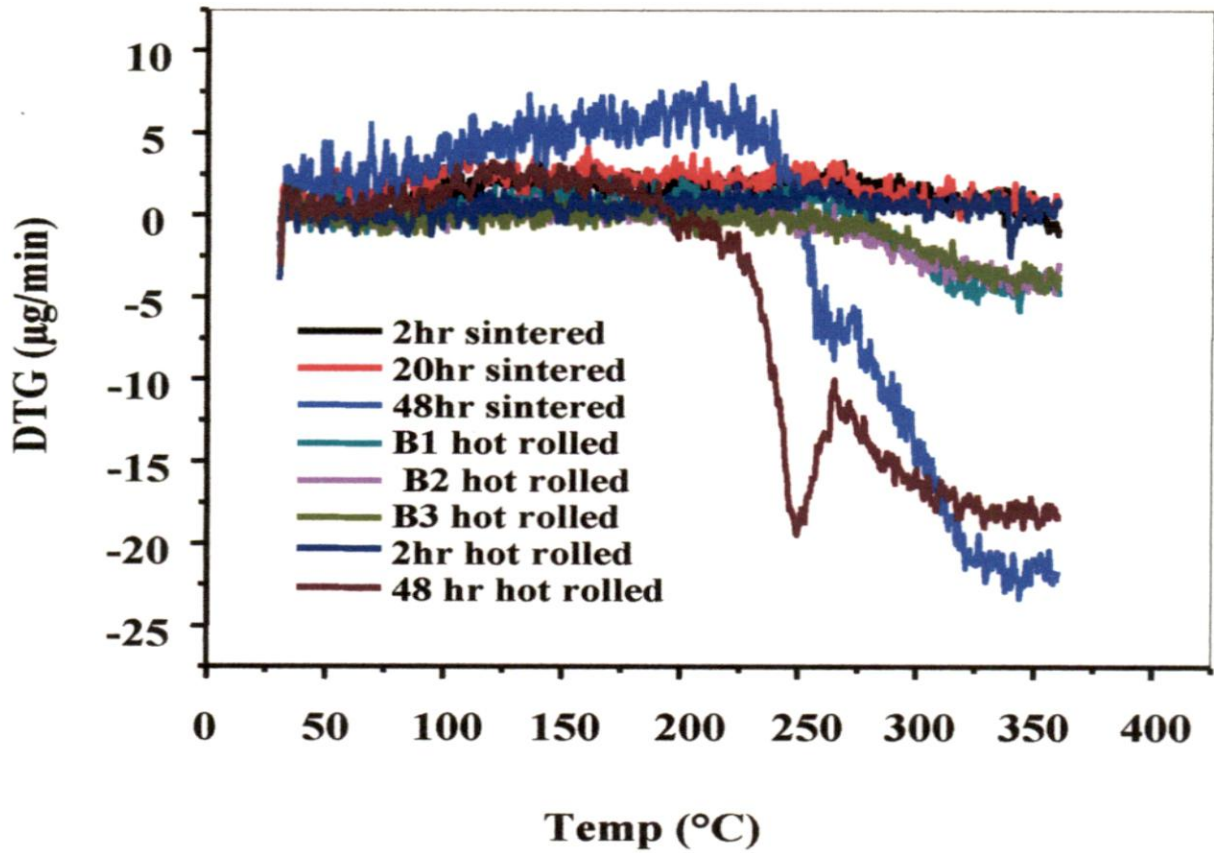


Fig: 4.11 f, g



4.11g.DTG Temp.Multiple Plot heating

Fig: 4.11g, h



4.18h. Phase Transformation Temperature Graph

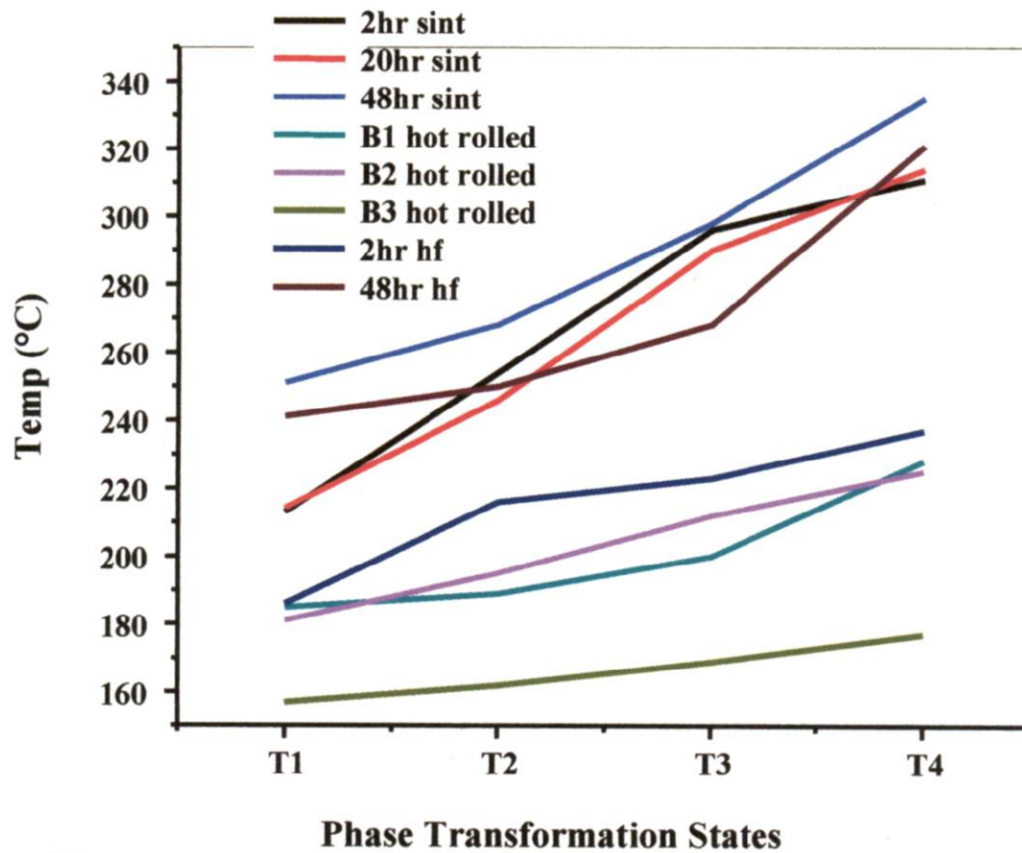


Fig: 4.11i

Table: 4.1i

	2hr	20hr	48hr	2hrhf	20hrhf	48hrhf	2hrhf	48hrhf
T1	213	214	251	185	181	157	186	241
T2	254	246	268	189	195	162	216	250
T3	296	290	298	200	212	169	223	268
T4	311	314	335	228	225	177	237	321

Table: 4.11j (T1, T2, T3, T4 are temperature of start of peak, highest point, finish

Time(hr) Temp(°C)	2hr	20hr	48hr	2hrhr	20hrhr	48hrhr	2hrhf	48hrhf
T2-T1	41	32	17	4	14	5	30	9
T3-T1	83	76	47	15	31	12	37	27
T4-T2	57	68	67	39	30	15	21	71

point and highest point of secondary peak.

For sharp exothermic peaks and maximum heat flow width of exothermic peak is minimum for 48 hr hot forged sample. Range of temperature between major and minor peaks is maximum for 48 hr hot forged sample. This observed phenomenon is desirable for maximum pseudoelastic effect, maximum strain. For nanocrystalline material synthesized by HEBM process, hot forging is better method to stabilize martensitic phase in material. After Thermomechanical training process two way shape memory effect can be developed and stabilized for large number of repeated cycles.

Chapter: 5 Conclusion

HEBM is a versatile processing method to fabricate nanocrystalline materials, relatively new for fabricating shape memory alloy material. No illustration has been found in this area to develop material by using HEBM method and process it further for fabricating devices which would exhibit enhanced SME. Here we have to face paradoxes regarding shape memory effect and nanocrystalline material. Shape Memory Effect is bulk transformation process where large change in volume takes place in thermodynamic cycling. Nanocrystalline powder is difficult to be handled for fabrication purpose in order to make a device which can be used for commercial purposes. In hot forging and rolling process nanocrystalline features lost significantly, enhanced mechanical properties, hardness, thermal stability does not remain invariant with further processing., this may be negative aspect for a specific case, otherwise this route of fabrication provides us variable range of transformation temperatures, based on this we can fabricate devices which can be used for different working conditions, i.e. at different temperature range.

Variation in transformation temperature range observed for various sample milled for different time periods. Thermomechanical training and milling time both have effect on transformation temperature and thus on shape memory effect.

Mechanical properties also changes with milling time. Hardness of material increases with reduction of particle size, governed by Hall Petch relation, to a certain point up to ~12nm size beyond that it decreases rapidly, this phenomenon is due to reverse Hall-Petch effect.

Materials which are difficult to process by conventional means can be processed by HEBM method and solubility limit can be increased beyond theoretical limit in this process.

Limitations are also there. We cannot have control in process parameters. We cannot have in-situ observation of mechanism of grain formation, refinement and atomic level movement in this process. HEBM needs further automation, incorporation of sensors along with high speed computing device to get control over process parameters so that we can get desired features.

Further work

We have observed difficulty to consolidate nanocrystalline powder material into solid device and retain nano features simultaneously by hot forging and rolling process. Research in this area is needed. Mechanism of severe plastic deformation in ball milling is highly statistical in nature; we don't have in-situ observation while process is going on. Automation is needed to have precise control over parameters during the milling process.

6. REFERENCES

- [1] S.Eucken (ed.). Bochum, DGM Information's Gesellschaft Verlag, 1992.
- [2] H. Tora Treatment thermique 234, France, 35, 1990
- [3] T. W. Duerig, K.N. Mrlton, D. Stockel, C.M. Wayman (Eds) London Butterworth Heinemann, 1990
- [4] Gh. Calugaru, L.G Bujorearu, S.Stancieu, I. Hopulele, R.Caliman, I Apachitei,Ed, Plumb Bacau Romania, ISBN 973-9150-50-0, 1950
- [5] Tadaki T (1948) In: Otsuka, Wayman CM (Eds) shape memory materials, Cambridge University Press.
- [6] Hussain S W, Clapp. PC (1987) J. Mater sci: 22:2351, doi: 10.1007/bf 01082115
- [7] Morris MA (1992) Acta Metal Mater sci 33:3579 doi: 10.1023/a: 10046477294
- [8] Gao Y. Zhu M, Lai JKL (1998) J Mater sci 33:3579, doi: 10.1023/A: 1004647127294
- [9] Li Z Pan ZY, Tang N, Ziang YB, Liu N, Fang M, Zheng M (2006) Mater sci Eng A 417:225
- [10] Z iao Z, Liz, Fang M, XiongS, Sheng X, ZHOU M(2008) Mater Sci Eng A 488:266
- [11] T.Saburi, C.M.Wayman, K.Takata, S.Nenno. Acta Metal, Matter. 28(1980)15.
- [12]R. Stallman. J. Vanhumbeek, L.Delaey, Acta Metal. Matter 28(1980) 15.
- [13] T. Tadaki, K. Otsuka, ISIJ Int. 29(5) (1989) 353.
- [14] S.Dutta, AK. Bhuniya, M.K. Banerjee, Mater. Sci.Eng. A300 (2001)
- [15] S. Bhattacharya, A.K. Bhuniya, M.K. Banerjee, Mater.Sci. Eng. Technology 9(1983) 654
- [16] J. Pons, E. Cesari, M. Rosca, Mater, Letr.9 (1990) 542
- [17] E. Cesari, C Piconnel, J. Pons, M.Sade, J. Phys.4 (Cu) (1991) 451
- [18] Schetky, L, L, L Mc, Shape-Memory Alloys Application, in J.H.Westbrook and R.L. Fleischer (Eds). Intermetallic compounds, vol, 2, Practice, New York: John Willey&sons, 1994
- [19] Wayman, C.M, Shape Memory Alloys, MRS Bulletin, 18, 1993
- [20] Carbon nanotechnologies, inc, Houston,TX, www.cnanotech.com [7] Wayman, C.M and Duerig,T.w, AN Introduction to Martensite and shape Memory, in T.W Duerig, K.N

Milton, D, Stocked, and C.W Wayman (Eds), engineering aspects of shape memory alloys, Butterworth-Heinmann, 1990, pp-452-469

[21] Delaney, I, Chandrasekhran, M, Andrade, M, and Van Humbeeck, J, Nonferrous Martensites, classification, crystal structure, morphology, microstructure, proceedings international conference. Solid state phase-transformation, Met. Society, of AMIE, PP, 1429-1453, 1999

[22] Maki, T, and Tamura, T, Shape Memory effect in Ferrous ALLOYS, Proc. ICOMAT-86, Japanese Institute of Metals, 1986, pp. 963-990

[23] Schwarz R Band Johnson W L (Ed) Solid State Amorphization Transformation, J. Less-Common Met. 140

[24] Shingu P H (Ed) 1992 Mechanical Alloying. Mater. Sci. Forum 88-90

[25] Johnson W L 1986 Prog. Sci. 30 81

[26] Fetch H J and Johnson W L 1988 Nature 334 50

[27] Fecht H J 1992 Nature 356

[28] Fecht H J, Hellstern E, Fu Z and Johnson W L 1990 Metall. Trans. A 21 2333

[29] Fecht H J, Hellstern E, Fu Z and Johnson W L 1989 Adv. Powder Metall. 1 111

[30] Bever M B, Holt D L and Titchener A L 1973 Prog. Mater. Sci. 17 5

[31] Meyers M A and Chawla K K 1984 Mechanical Metallurgy (Englewood Cliffs, Nj: Prentice-Hall) p 494

[32] Karch J, Birringer R and Gleiter H 1987 Nature 330 556

[33] Fecht H J 1990 Phys. Rev. Lett. 65 610

[34] Feynman, R, There's Plenty of Room at the Bottom, Annual Meeting of the American Physical Society, December 29, 1959, Caltech Engineering and Science, February 1960.

[35] Schetky, L, L, L. Mc. The Present Status of Industrial Application FOR Shape Memory Alloys; Proceedings: Shape Memory Alloys for Power Systems, Palo Alto, CA, 1994, PP. 4.1-4.11.

[36] Jacson, C.M, Wagner, H.J., and Wasilewski, R.J., NASA Report SP-5110, Washington, D.C., 1972, pp. 74, 78, 79.

[37] Miyazaki, S., Ishida, A., Martensitic Transformation and Shape Memory Behavior in Sputter-Deposited Ti-Ni-Base Thin Films, Material Science and Engineering, A273-275, 1999, pp. 106-133

[38] Stockel, D., Adv. Mater. Process., October 1990, pp. 35, 38.